Research Paper

GEOSPHERE

GEOSPHERE, v. 17, no. 5

https://doi.org/10.1130/GES02376.1

15 figures

CORRESPONDENCE: brucel@earth.ox.ac.uk

CITATION: Levell, B., Searle, M., White, A., Kedar, L., Droste, H., and Van Steenwinkel, M., 2021, Geological and seismic evidence for the tectonic evolution of the NE Oman continental margin and Gulf of Oman: Geosphere, v. 17, no. 5, p. 1472–1493, https://doi.org/10.1130/GES02376.1.

Science Editor: David E. Fastovsky
Associate Editor: Andrea Fildani

Received 29 November 2020
Revision received 23 February 2021
Accepted 11 May 2021

Published online 19 August 2021

Geological and seismic evidence for the tectonic evolution of the NE Oman continental margin and Gulf of Oman

Bruce Levell[1], Michael Searle[1], Adrian White[1,*], Lauren Kedar[1,†], Henk Droste[1], and Mia Van Steenwinkel[2]

[1]Department of Earth Sciences, University of Oxford, South Parks Road, Oxford OX1 3AN, UK
[2]Locquetstraat 11, Hombeek, 2811, Belgium

ABSTRACT

Late Cretaceous obduction of the Semail ophiolite and underlying thrust sheets of Neo-Tethyan oceanic sediments onto the submerged continental margin of Oman involved thin-skinned SW-vergent thrusting above a thick Guadalupian–Cenomanian shelf-carbonate sequence. A flexural foreland basin (Muti and Aruma Basin) developed due to the thrust loading. Newly available seismic reflection data, tied to wells in the Gulf of Oman, suggest indirectly that the trailing edge of the Semail Ophiolite is not rooted in the Gulf of Oman crust but is truncated by an ENE-dipping extensional fault parallel to the coastline. This fault is inferred to separate the Semail ophiolite to the SW from in situ oceanic Gulf of Oman crust to the NE. It forms the basin margin to a "hinterland" basin formed atop the Gulf of Oman crust, in which 5 km of Late Cretaceous deep-water mudstones accumulated together with 4 km of Miocene and younger deep-water mudstones and sandstones. Syndepositional folding included Paleocene–Eocene folds on N-S axes, and Paleocene to Oligocene growth faults with roll-over anticlines, along the basin flank. Pliocene compression formed, or tightened, box folds whose axes parallel the modern coast with local south-vergent thrusts and reversal of the growth faults. This Pliocene compression resulted in large-scale buckling of the Cenozoic section, truncated above by an intra-Pliocene unconformity. A spectacular 60-km-long, Eocene(?) to Recent, low-angle, extensional, gravitational fault, down-throws the upper basin fill to the north. The inferred basement of the hinterland basin is in situ Late Cretaceous oceanic lithosphere that is subducting northwards beneath the Makran accretionary prism.

INTRODUCTION

The Oman Mountains spectacularly document the Late Cretaceous obduction of the Semail Ophiolite complex and underlying thrust sheets of Neo-Tethyan oceanic rocks (Haybi and Hawasina complexes). This obduction was from northeast to southwest over the Permian–Mesozoic carbonates of the Arabian shelf or platform (Glennie et al., 1973, 1974; Searle, 2007). Restoration of the thrust sheets records several hundred kilometers of shortening in the Neo-Tethyan continental margin to slope (Sumeini complex), basin (Hawasina complex), and trench (Haybi complex) facies rocks during ophiolite emplacement (Searle, 1985, 2007; Cooper, 1988; Searle et al., 2004). The present-day southwestward extent of the ophiolite and Hawasina complex thrust sheets is at least 150 km across the Arabian continental margin. The obduction, which spanned the Cenomanian to Early Maastrichtian (ca 95–72 Ma; Searle et al., 2004; Searle, 2007), resulted in flexure of the crust and formation of the Late Cretaceous Muti and Aruma foreland basin, southwest of the advancing thrusts (Fig. 1: Robertson, 1988; Robertson 1987a, 1987b; Boote et al., 1990; Warburton et al., 1990; Ali and Watts, 2009; Ali et al., 2013; Ali et al., 2020). A negative Bouguer gravity anomaly in the "Sohar basin" offshore north Oman was interpreted to be the response of a Late Cretaceous and Cenozoic sedimentary basin at least 10 km thick (Ravaut et al., 1997, 1998). This "hinterland" basin (Mann et al., 1990) appears to be volumetrically similar in size to the foreland basin but is narrower, deeper, and has currently active (gravitational) faulting. The onshore record of this basin is restricted to patchy outcrops along the Batinah Plain (Fig. 2) of latest-Cretaceous deep-water sediments. Shallow-marine Paleocene–Eocene limestones unconformably overlie these sediments and onlap all older units (Glennie et al., 1974; Mann et al., 1990). These rocks are exposed all around the large (60-km-wavelength) Jebel Akhdar and Saih Hatat anticlines (Searle, 2007). Along the southwest flank of these mountains, these rocks show northwest-southeast–aligned fold axes indicating minor, Late Eocene or younger, northeast-southwest shortening. In the coastal region around Muscat, between Ras al Hamra and Bandar Khayran (Fig. 2), these Paleogene rocks show large-scale box folds that have axes aligned north-northwest–south-southeast almost at right-angles to the Late Cretaceous fold trend (Fournier et al., 2006).

Although the geometry and timing of the onshore Late Cretaceous thrust sheets and the stratigraphy of the post-obduction latest-Cretaceous clastic and Paleocene–Eocene limestone cover are well known, the northeastern extent of the onshore geology into the Gulf of Oman (also known as the Sea of Oman) remains poorly known. Major tectonic questions concerning this basin remain, including: (1) Is the Semail ophiolite thrust sheet rooted into the Gulf of Oman crust, or is it detached? (2) What was the cause of the variously oriented compressional anticlines formed during the Cenozoic? (3) What is the geometry

Bruce Levell https://orcid.org/0000-0002-7414-1565
*Now at British Geological Survey, Keyworth, Nottingham, NG12 5GG, UK
†Now at School of Earth Sciences, University of Aberdeen, Aberdeen, AB24 3FX, UK

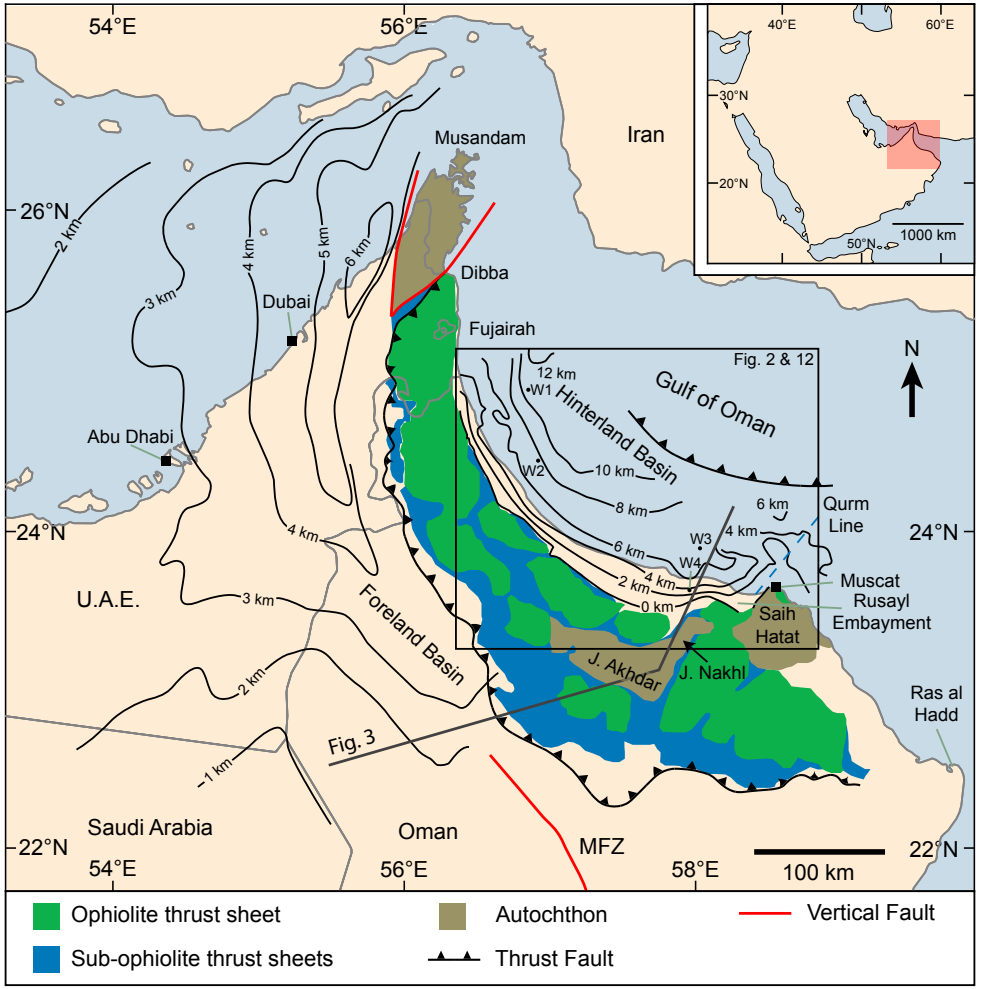

Figure 1. Study area and structural map with contours in km below sea level of the depths to the base of the Foreland Basin and Hinterland Basin. In both cases, the contours are on surfaces close to the base of the post-obduction sedimentary sequences. In the composite Fiqa/Pabdeh/Fars Foreland Basin to the west, the mapped surface is close to the Wasia/Aruma break (Fig. 3) and is based on the Top-Thamama map of Boote et al. (1990) and the Natih "E" map of Terken (1999). Note that the Foreland Basin extended all the way to the southeast along the frontal thrust, including to the east of the Maradi fault zone (MFZ). The area east of the MFZ has suffered late (Plio-Pleistocene) uplift (Filbrandt et al., 2006) on the order of 1 km or less. Irrespective of later uplift, the foreland basin clearly has a depocenter to the north in the United Arab Emirates (UAE) (Ali and Watts, 2009; Ali et al., 2013). The Hinterland Basin structural contours are minimum depth estimates of the base of the post-obduction sediments (Late Campanian and younger), based on seismic data in this study. Note that the Hinterland Basin contour interval is 2 km and that this basin is both substantially deeper and narrower than the Foreland Basin. The well locations used in this study are shown (black dots: three offshore and one onshore). The black box is the area of the maps in Figure 12.

of the offshore Oman hinterland basin, and how does its deformation history relate to the poorly constrained Cenozoic onshore deformation? (4) What was the geometry of the northern margin of the continental portion of the Arabian plate? The Semail ophiolite, by definition, is that section of Late Cretaceous oceanic crust and upper mantle obducted onto and underlain by Arabian continental crust, whereas any "Gulf of Oman oceanic crust" is in situ and not underlain by continental crust. Thus, it is important to ascertain how far offshore the continental basement extends beneath the overlying Cenozoic rocks.

This paper presents new data concerning the connection between the onshore and offshore geology along the northeast coast of Oman. We constrain solutions to these questions by combining the onshore outcrop geology with offshore data acquired since the work of Ravaut et al. (1997), namely seismic reflection data and well data. Our study area extends from Sohar to Muscat and the adjacent offshore area in the Gulf of Oman (Fig. 1). To the north, the United Arab Emirates (UAE) onshore-offshore has been studied by Ali et al. (2020). The eastern boundary of the study areas is the north-south–aligned "Qurm line" (Fig. 2; new name). This geological boundary in the offshore, west of Muscat, delimits the Saih Hatat metamorphic rocks and Muscat ophiolite to the east from the Batinah coast-type hinterland basin geology to the west. This boundary is related by Ninkabou et al. (2021) to the Semail fault zone

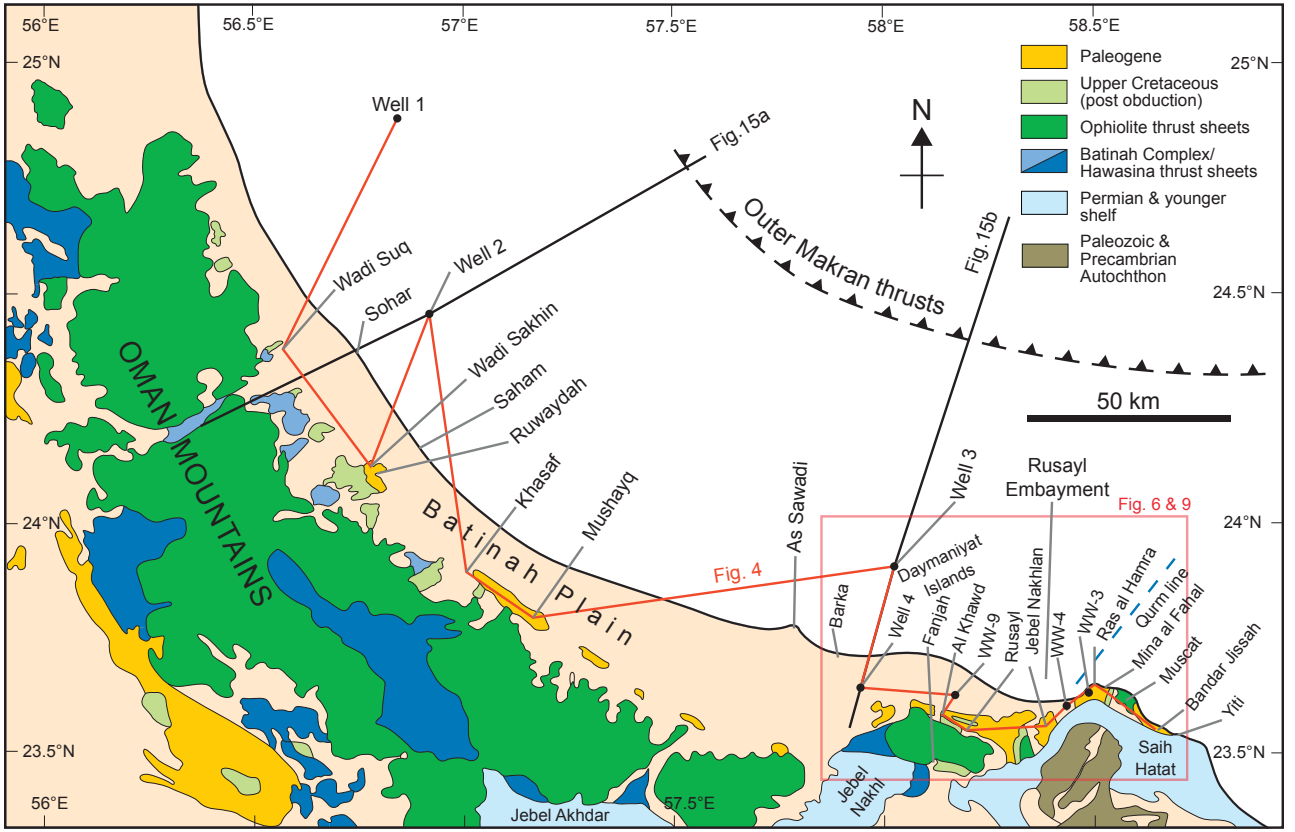

Figure 2. Locations of study areas, places mentioned in the text, and cross sections.

structure (Glennie et al., 1974; Robertson and Searle, 1990; Scharf et al., 2019) and, addressing point 4 above, to a promontory in the continental margin of Oman offshore Muscat. Ninkabou et al. (2021) complement our work by addressing the offshore seismic data immediately to the east of our study area, tied to data from Well 3 in this paper. Ninkabou et al. (2021) also include line interpretations of two regional seismic lines from the southern portion of our study area.

WESTERN GULF OF OMAN GEOPHYSICS

The majority of published geophysical work in the Gulf of Oman has been done east of Ras al Hadd (59°48′E) and has focused on unravelling the plate interactions between the Asian, Indian, and Arabian plates along the Makran subduction zone, the Murray Ridge, the Owen fracture zone, and the eastern Oman margin (e.g., Rodriguez et al., 2016, and references therein). We are here concerned with an area well to the west and particularly the area between Musandam and Muscat (Fig. 1).

Ravaut et al. (1997, 1998) used a data set comprising 15 regional 2D seismic lines and regional satellite gravity data, together with three offshore wells: (Wells 2 and 3 and Fujairah-1). The seismic data were reconnaissance, shot in a zig-zag, and at best defined a very loose 100 km grid. Uchupi et al. (2002) reported on four of the same lines. Ravaut et al. (1998) defined the "Sohar Basin," an area of thick sedimentary cover between Musandam, Muscat and a supposed basement ridge ("Saih Hatat–Musandam ridge"), roughly 50 km from the coast (i.e., halfway across the Gulf of Oman to the frontal thrusts

of the Makran accretionary wedge). This structure was based only on gravity data, and Ravaut et al. (1997) pointed out that it needed confirmation from better seismic data. Ravaut et al. (1998) interpreted a profile offshore south of Sohar on the Batinah Coast (Fig. 2) as showing that the Oman continental crust thinned from 38 to 40 km onshore to 20 km or less in the Gulf of Oman, with an unrooted edge to the 5–7-km-thick onshore ophiolite slab near the present-day coastline. In this model, thinned continental crust extends some 40 km offshore under the Gulf of Oman before transitioning to oceanic crust. Ravaut et al. (1997) extended this analysis using 3D modeling of the complicated flexural loads, and they concluded that the continental crust with the Moho at ~20–24 km could extend under the Gulf of Oman all the way to the Makran trench. In this paper, we show, with the benefit of considerably more seismic data, that the inferred basement ridge (Saih Hatat–Musandam ridge) does not exist, and that the "Sohar Basin" sedimentary fill is contiguous with the sedimentary fill that is affected by imbricate thrusting in the inner trench wall of the Makran subduction zone. The "Sohar Basin" as defined by Ravaut et al. (1998) is thus simply the western part of what we would prefer to call the "Western Gulf of Oman Basin" (WGOB).

In the eastern Gulf of Oman, seismic-refraction results from the area west of 61°E show that the crust is oceanic. North and east of Ras al Hadd, heat-flow measurements have been used to suggest an age of 100–70 Ma for this oceanic crust (White and Ross, 1979; Hutchison et al., 1981). No refraction data have been published west of Ras al Hadd. Speculations as to the nature of the crust in the study area are currently based solely on the surrounding geology, bathymetry, and gravity data.

To the northwest of our study area, offshore Fujairah, Ali et al. (2020) acquired seismic reflection data onshore and offshore, receiver function analysis, gravity data, and offshore seismic reflection data. They were unable to resolve the relationship between the Gulf of Oman crust and the ophiolite but argued for a low-angle extensional fault dipping east-southeast separating the thick offshore Late Cretaceous and younger sediments from the top ophiolite, and, at depth, detaching the (unrooted) ophiolite from the Gulf of Oman crust. They deduced that the latter is oceanic based on thickness (~10 km of crust below 10 km of sediment) and on its loading behavior, as revealed by back-stripping the well data.

Across the WGOB, Ninkabou et al. (2021) present two regional seismic lines that were tied to Well 3 (with data summarized in a graphical log). Much of their work, however, was done farther to the east, in the offshore Hatat and Tiwi basins. As they highlight, these basins, which lack any well data, are separated from our study area by a clear geological boundary, which they interpret as the offshore extension of the Semail fault zone (Fig. 1).

WESTERN GULF OF OMAN GEOLOGY

Eight wells have been drilled offshore in the Western Gulf of Oman Basin, and one has been drilled onshore. Four of these wells are offshore Fujairah (ERF-1, Fujairah 1, 2, and FMA-1) and two off Omani Musandam (Dibba-1 and Musandam-1). Ricateau and Riché (1980) discuss the geology offshore Fujairah. In our study area (Fig. 1), there are three offshore wells from north to south: Well 1 (drilled in 2009; total depth [TD] 3232 m), Well 2 (drilled in 1968; TD 4014 m), and Well 3 (drilled in 1971-2; TD 4630 m). All three reached TD in Late Cretaceous deep-water mudstones. None penetrated any form of basement.

Ravaut et al. (1997) also recognized that the fill of the "Sohar Basin," which they also regarded as mostly post-obduction (i.e., Late Campanian and younger), was divided temporally into two phases of subsidence: Cretaceous to Early Miocene (or Oligocene in the north near Sohar) and Late Miocene and younger. The base of the sediments was too deep to be mapped on the then-available seismic data, but on gravity data, it was interpreted as ranging from 7.5 km (off Sohar) to 9 km depth farther south, and up to 10 km along the hanging wall of the Makran fold and thrust belt. Al Anboori (2004) presents the most detailed published analysis of the geology and hydrocarbon prospectivity of the Oman offshore between Sohar and Muscat. The paper includes geological cross sections, calibrated by unpublished well data. It is based on seismic-reflection lines illustrating the major growth-fault systems affecting the thick Cenozoic section.

ONSHORE GEOPHYSICS

Manghnani and Coleman (1981) used data from 460 new gravity stations in four profiles, one of which, through Muscat, was extended offshore using marine data from White and Ross (1979). This 325-km-long line was modeled as showing a 42-km-thick continental crust passing into a 16–18-km-thick oceanic crust. They concluded that the Muscat ophiolite (peridotite) thrust sheet, modeled as some 5–7 km thick, 50 km wide, and with a 35° dip to the north, flattening rapidly offshore, was not rooted in the mantle (their figure 6).

Shelton (1990) used 900 newly acquired gravity stations, Petroleum Development (Oman) Ltd. (PDO) gravity surveys, and onshore seismic data to constrain the gravity solution for the geometry of the ophiolite under the Batinah plain. The data were in part published as a map in Lippard et al. (1986). He concluded that the ophiolite, in aggregate, formed a flat-based wedge disconnected from both Gulf of Oman crust and the upper mantle. His gravity models show an ophiolite pinch-out line very close to the present-day coast, and he cited seismic and geological indications, for at least the Fizh and Sarami ophiolite blocks near Sohar, that the line of termination was a low-angle normal fault or faults dipping northeast. Shelton (1990) computed a maximum thickness of the ophiolite slabs of 6 km, in good agreement with outcrop measurements by Mann et al. (1990) and Nicolas et al. (1996). This work shows that the Batinah plain is underlain by ophiolite slabs with the upper surface dipping at 30° toward the coast in the north, flattening southeastward to 15° in the Jebel Nakhl area. The slab thins to zero at the coast near Sohar and somewhat farther landward than the coast in the Barka area (Fig. 2) (Shelton, 1990; his figure 5: the zero mgal residual anomaly). He modeled the base of

the ophiolite as flat, which was both a convenient modeling assumption and regarded as a good fit to the geology.

Al Lazki et al. (2002) published a composite regional 2D seismic line, receiver function data, and information from 15 onshore wells including Well 4. The preferred model (Model A) favors a thick continental crust, 42 km near the coast, thickening to an exceptional 48–51 km under Jebel Akhdar. The Nakhl ophiolite block was modeled as 5–8 km thick with a wedge geometry on its trailing edge, tapering rapidly toward the coast. This is similar to the gravity-modeled geometries of both Manghnani and Coleman (1981) and Shelton (1990). It was also modeled as continuing offshore as a <1-km-thick body for 30 km or more beyond the coast. The well-imaged top ophiolite at Well 4 was shown to be planar and dipping at 15° north-northeast, in accordance with the results of Shelton (1990) and the onshore seismic line that they published.

ONSHORE GEOLOGY

The key area for establishing a connection between on and offshore geology is the Rusayl Embayment (Fig. 2; red box) between Jebel Nakhl and Saih Hatat. Together with the scattered outcrops of Campanian to Maastrichtian Thaqab Formation near Sohar, this area provides the best exposures of the relevant post-obduction sequence. Thicknesses and age data for the post-obduction sequences of these areas are summarized in Figures 3 and 4. Nolan et al. (1990) summarized and formalized the stratigraphy in these areas, based also on observations by Villey et al. (1986 a, 1986b) and Le Métour et al. (1986) in monographs accompanying the Omani geologic maps (also summarized by Rabu et al., 1993). Mann et al. (1990) described scattered outcrops of the post-obduction Cretaceous sequence of the Batinah plain, which is thick (more than 1 km) and consists of deep-water facies including turbidites and debris flows. In the northern onshore area toward Sohar, Woodcock and Robertson (1982) and Robertson and Woodcock (1983) described the problematic Batinah Complex. These supra-ophiolite thrust sheets of Mesozoic rocks belong to a distal passive margin area. They are faulted against Campanian to Maastrichtian deep-water deposits of the post-obduction Late Cretaceous hinterland basin and appear to be part of its basement. Mann et al. (1990) noted the presence of a prominent, continuous, down-to-the-coast faulted contact separating post-obduction cover from its basement (namely, the autochthon, sub-ophiolite thrust sheets, the ophiolite, and the Batinah Complex). Structural style varies along this lineament (named the "Batinah Coastal Fault" by Mattern and Scharf, 2018, it runs 10–20 km inland) but includes low-angle normal faults (e.g., at Ruwaydah). Combining the results of Shelton (1990) and Mann et al. (1990), there is therefore a case to be made that the seaward-dipping upper surface of the ophiolite wedge is either a low-angle, northeast-dipping extensional fault, or there is a low-angle extensional fault in the overburden set up by the simply dipping top surface of the ophiolite. Mann et al. (1990) appear to have been the first to use the term "hinterland basin" for the WGOB, explicitly comparing it with the older Aruma (Fiqa) and younger (Pabdeh) foreland basins south and west of the mountains (Figs. 1 and 3).

Coffield (1990) mapped the ophiolite and immediately underlying and overlying rocks in the Rusayl-Fanjah area. Post-ophiolite sediments (? Maastrichtian to Eocene) are folded into upright folds with north-south axes as a result of compression attributed to the uplift of the two flanking culminations of Saih Hatat and Jebel Nakhl. A similar observation that the fold structures and orientations in the Paleogene of the Rusayl embayment were fundamentally constrained by the Saih-Hatat and basement structures in the embayment itself was made by Glennie et al. (1974) and Mann et al. (1990).

Fournier et al. (2006) reviewed the structural geology of the exposed Paleogene rocks, primarily in the area between Muscat and Sur. They used fractures and fault orientations as stress indicators. Through a process of stress inversion, these were reduced to principal stress directions. Based on families of common inferred stress directions, regional conclusions about tectonic phases during the Cenozoic were drawn. However, as noted by previous workers, at least in the Rusayl embayment, the basement structures have exerted major control on local fold geometries. Hence, in many areas, the fracture-derived principal stress directions, particularly those close to the major structures, must be local. With this caveat, Fournier et al. (2006) suggested a complex history of three main regional phases: (1) Late Cretaceous to Early Eocene east-northeast–west-southwest extension; (2) post-Eocene, renewed east-northeast–west-southwest extension followed by north-northeast–south-southwest extension; (3) Early Miocene–Pliocene inversion and compression, initially oriented east-west to northeast -southwest followed by a later phase oriented north-south to north-northeast–south-southwest.

DATASET AND METHODS

The seismic data available to this study included surveys by Digicon (1989), Western Geophysical (1999), and PGS (2002), much of which was reprocessed in 2011, including an approximate 5 km grid of 36 lines covering an area of 70 × 50 km between the Daymaniyat Islands and Qurm. The greater part of the study area is covered by an additional roughly 5 km grid in a 20-km-wide offshore strip between Sohar and Well 3, and an ~20 km grid, together comprising 113 lines over the rest of the larger study area (Fig. 1). Depth conversion (Fig. 5) is based on check-shot velocity data from Wells 2 and 3, extrapolated beyond TD with stacking velocities (as presented by Calvache and Love, 2001). The apparent lack of compaction-related velocity increase below 4 km is suggestive of overpressure in the Late Cretaceous sequence. Direct well-to-seismic correlation is problematic due to severe thinning over growing syndepositional anticlines and fault cut-outs. Our correlations between onshore and offshore are therefore based on (1) extrapolation away from the key Well 3 in the Rusayl area and Well 1 in the north; (2) the geological events revealed by the stratigraphic data from the onshore outcrops and wells; and (3) structural extrapolation using dips and thicknesses from onshore to offshore (Fig. 5).

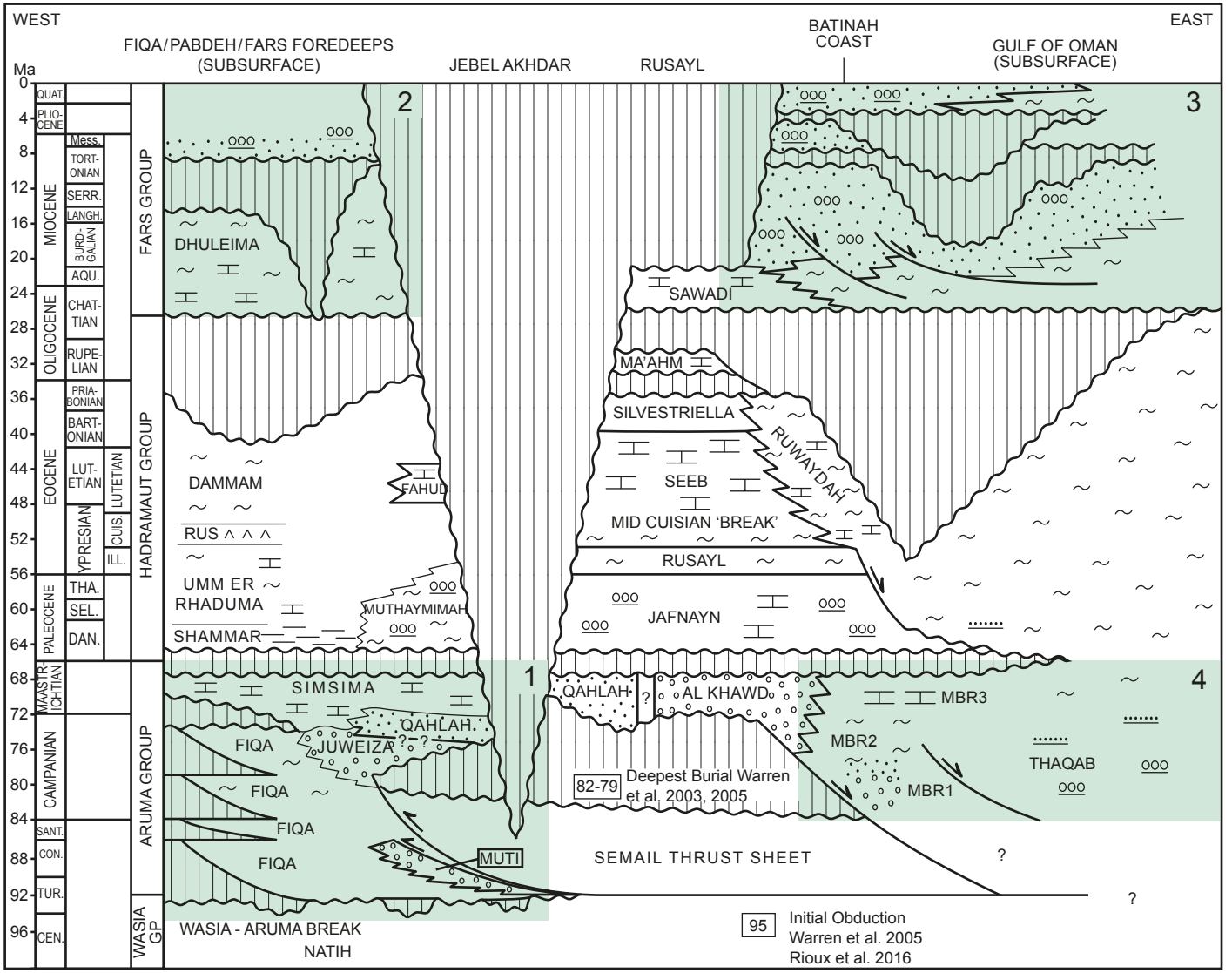

Figure 3. Chronostratigraphic chart of the post-obduction basins on either side of the Oman Mountains (Fig. 1). Four depocenters (1–4) are represented in this diagram. (1) In the west, the Fiqa basin is a flexural foreland basin, which began to form in the Coniacian (Boote et al., 1990) exterior to the thrust loads of the obduction complex (i.e., the Sumeini, Haybi, Hawasina, and Semail thrust sheets), emplaced by 79 Ma (intra-Campanian). This basin is infilled with 2–4 km of deep-water and slope deposits derived largely from the thrust pile (Warburton et al., 1990). In the north (United Arab Emirates [UAE]), this basin fill is overlain by a second flexural foreland basin fill (2)—the Pabdeh/Fars basin in the Mio-Pliocene (Boote et al., 1990; Ali and Watts, 2009; Ali et al., 2013), which is related to the thrusting and arching of the Musandam nappes. Both of these successions are associated with syndepositional thrusting. These basins are together outlined by the structural contour map at top Thamama/Natih "E" levels in Figure 1. To the east along the Batinah Coast and in the Gulf of Oman, there are also two phases of thick deposition. The oldest (3) is the Campanian to Maastrichtian Thaqab Formation (Nolan et al., 1990) and its offshore equivalents: a 4–5-km-thick stack of deep-water and slope deposits derived from the uplifted thrust sheets. The youngest (4) is a 4–5-km-thick Mio-Pliocene succession of sands, gravels, and marls (Figs. 12C and 12D), age-equivalent to the 3-km-thick Fars Group west of the Mountains. Both successions are associated with syndepositional extensional faulting. The minimum depth to the base of these successions, together with the relatively thin intervening Paleogene succession, is outlined in Figures 1 and 12A. Based on Glennie et al. (1974); Le Métour et al. (1986); Villey et al. (1986a, 1986b); Mann et al. (1990); Nolan et al. (1990); Skelton et al. (1990); Warburton et al. (1990); Racey (1995); Forbes et al. (2010).

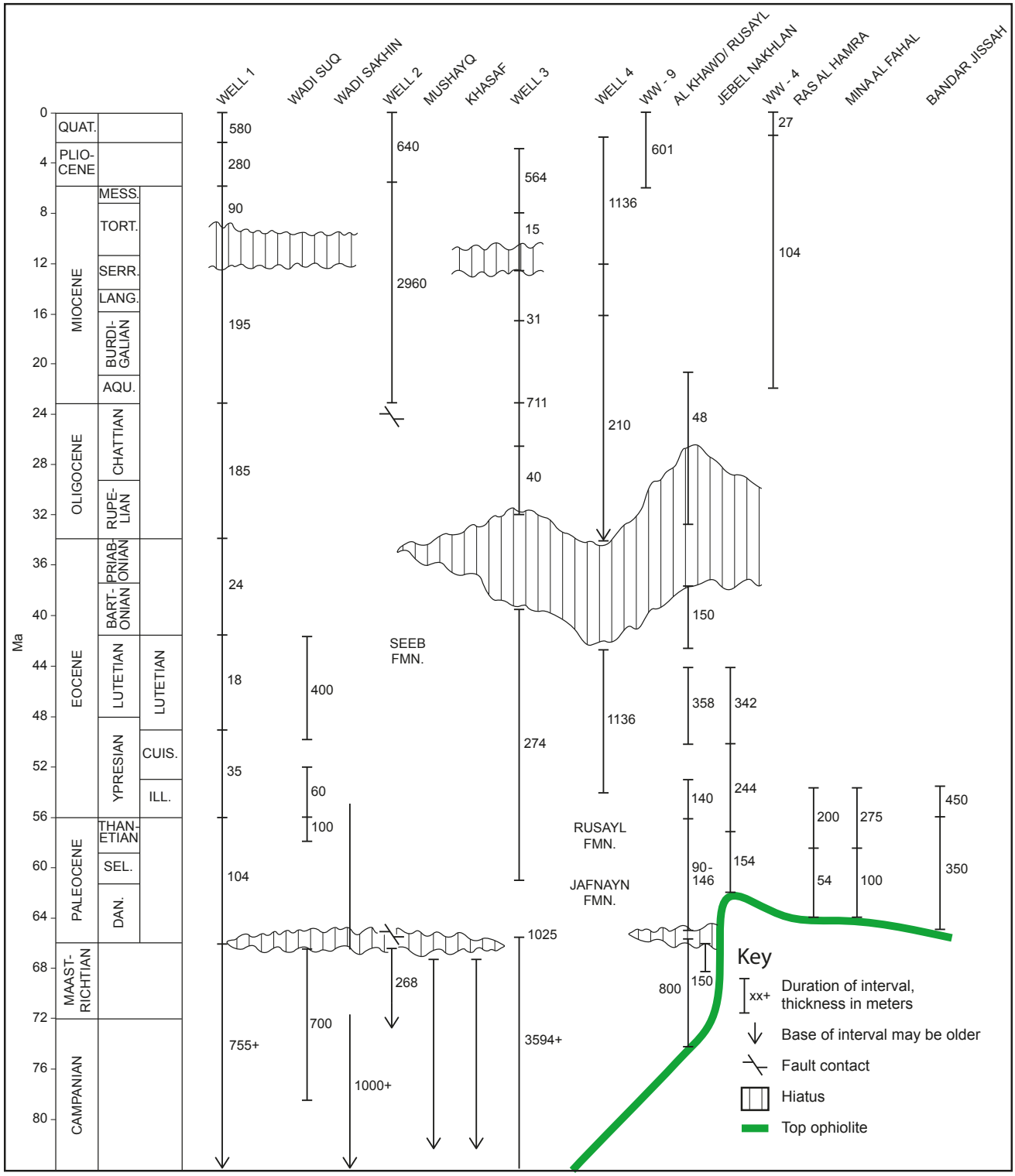

Figure 4. Chronostratigraphic chart of the Western Gulf of Oman Basin (WGOB) along the NE Oman coast: Rusayl Embayment and Muscat areas. For locations, see Figure 2. Numbers are thicknesses in meters. Note that the two thickest intervals are the Late Cretaceous and Mio-Pliocene. Based on confidential reports and Le Métour et al. (1986); Rabu et al. (1986); Villey et al., (1986a, 1986b); Mann et al. (1990); Nolan et al., (1990); Racey (1995); and Abbasi et al. (2014).

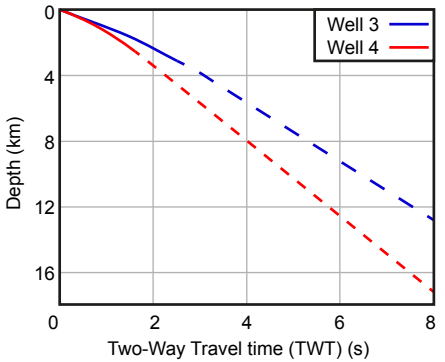

Figure 5. Two-way travel time (TWT) versus depth curves used for the depth conversion of offshore seismic data based on Wells 2 and 3, extrapolated beyond the deepest point of the wells, with stacking velocities (Calvache and Love, 2001).

ONSHORE-OFFSHORE CORRELATION (RUSAYL EMBAYMENT AND ADJACENT OFFSHORE)

The offshore well data are insufficient on their own to constrain the ages of some of the horizons in our seismic interpretation. In this section, we therefore present the evidence for the expected reflection character of the formations and key stratigraphic horizons. This is to support our preferred correlations from the Rusayl Embayment area onshore to the offshore 2D seismic grid. We also provide, in stratigraphic order, the depositional context of the Late Cretaceous WGOB. The offshore well data are all based on confidential company reports and not the authors' own work or direct observations.

Late Cretaceous: Onshore

The margins of the Rusayl Embayment (Fig. 2) are defined by the "Frontal Range fault" (Hanna, 1990; Mattern and Scharf, 2018). This is a series of connected normal faults that juxtapose, by virtue of the km-scale footwall uplift, the autochthon plus remnants of the allochthonous Hawasina and Semail Ophiolite thrust sheets against the onlapping post-obduction Late Cretaceous to Oligocene sequence. The highest structural levels of the sub-ophiolite autochthonous sequence on the northern flank of Saih Hatat are carbonates of the Triassic Akhdar Group (Mahil Formation). They are locally overlain by Early Jurassic (Sahtan Group) carbonates and minor sandstones up to a few hundred meters thick (Villey et al., 1986a, 1986b). The surface of the autochthon along this entire flank is widely mylonitized, including a "marble" horizon of mylonitized Early Jurassic carbonates, containing *Lithiotis* at Bausher.

The basement of the western flank of the Rusayl Embayment, at Jebel Nakhl (Fig. 6), is similar, except that there is preservation of the younger Kahmah Group and lowermost Wasia Group. This is represented by the so-called Al Hassanat Formation, which is the Upper Aptian to lowermost Middle Albian platform-margin facies equivalent of the Nahr Umr Formation (Masse et al., 1997). It is therefore likely that the top of the sub-ophiolite autochthonous sequence gets younger from Jurassic to Early Cretaceous across the Rusayl Embayment and that, if seismically imaged, it would consist of an abrupt, flat-topped, well-bedded, seismically fast, platform sequence, possibly thicker to the west, and underlain by the base-Permian angular unconformity.

None of the distinctive geometries or surfaces described above are recognized on the offshore seismic data. This is taken as important negative evidence: i.e., that the seismic data are not imaging the deeper structural levels of top ophiolite or top autochthon. Correlation with the offshore is therefore based on the onshore post-obduction Campanian to Maastrichtian sequence. The Late Campanian to Late Maastrichtian Al Khawd Formation at Al Khawd (or Al Khod) in the Rusayl Embayment is 650 m thick according to Abbasi et al. (2014), 800 m according to Schulp et al. (2000), and just 150 m 10 km to the east, at Rusayl (Villey et al., 1986b). The formation rests disconformably on, and is faulted against, the ophiolite. The age is based on ornithischian and turtle bones (Schulp et al., 2000). The formation is interpreted as fluvial, based on the terrestrial to shallow-water fauna and the presence of (lateritic) paleosols. Paleocurrents are predominantly to the north-northeast in the Al Khawd area (Abbasi et al., 2014). The formation is reddish-brown and conglomeratic but has a widely varying content of mudstone and conglomerate and differs in clast content, conglomerate percentage, thickness of interbedded mudstone, and consolidation in each of its outcrop areas. Abbasi et al. (2014) concludes that the lithologic and facies variability is due to a variety of local drainage systems being represented in the one formation. Both Nolan et al. (1990) and Abbasi et al. (2014) document an inverted stratigraphy of detrital clasts in the Al Khawd Formation, which is testimony to contemporary uplift of the Saih Hatat area with erosion down to Cambro-Ordovician levels. Farther to the southeast, Nolan et al. (1990) and Abbasi et al. (2014) describe sections of the partially time-equivalent Qahlah Formation (Fig. 3) around the uplifted Jebel Nakhl and Saih Hatat structures. At the base, laterites developed directly on the ophiolite erosion surface, and the lower units are largely polymict fluvial conglomerates. The characteristics of the Al Khawd, and the fluvial parts of the Qahlah Formations, imply that units of similar age and facies, if present offshore, would rest on an erosional unconformity, have a variable thickness, and display highly variable frequency and reflection continuity on seismic data.

The upper part of the Qahlah Formation includes shallow-marine *Loftusia*-bearing Maastrichtian limestones. Similar Maastrichtian limestones, 237 m thick and similar to the Simsima Formation in the northern Oman Mountains, are also reported on the Batinah plain (Nolan et al., 1990). The Simsima Formation, if present offshore as a marine equivalent of the Al Khawd Formation, would probably not be distinctive. It might be expected to have a parallel continuous reflection character.

Outside the Rusayl Embayment, but important here because of relevance to offshore Well 3 discussed below, the Thaqab Formation and the locally underlying Rawdah Conglomerate (Fig. 2; Nolan et al. 1990) outcrop in faulted inliers along the Batinah plain. They are up to 1 km thick, structurally above the Semail ophiolite and the Batinah Complex (Nolan et al., 1990). Mann et

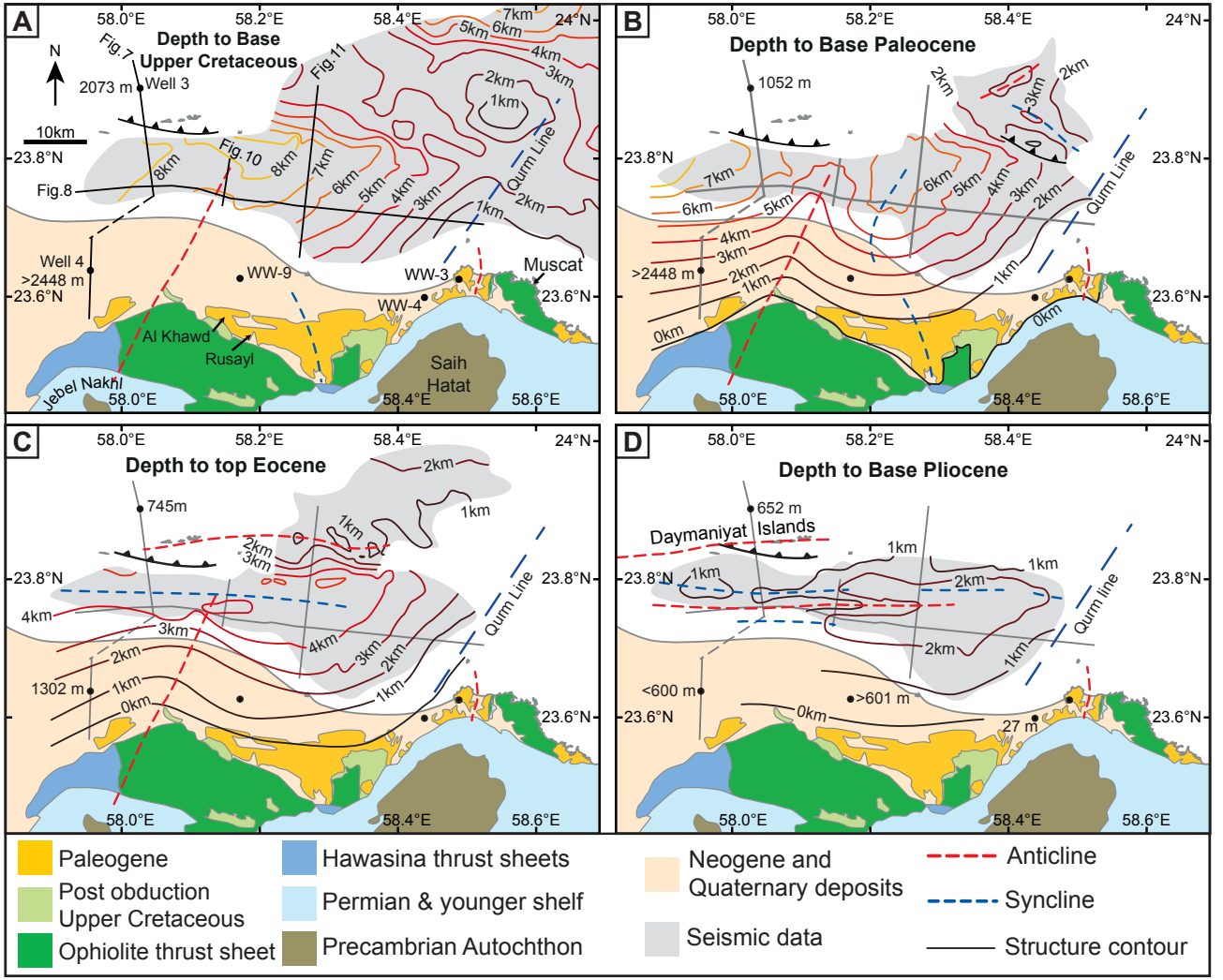

Figure 6. Structural contour maps of horizons in the Rusayl Embayment and adjacent offshore (for location, see red box in Fig. 2). The gray area is the extent of the mapped seismic data used in each map. (A) "Base Upper Cretaceous" structure contour map. There are no well penetrations or ties to this horizon. The map represents the deepest mappable event on seismic (blue in Figs. 7, 8, and 11), above which there was conformable sedimentation to the present, and it is therefore interpreted as near the base of the post-obduction sequence. However, the map represents a minimum depth to this surface because there is no clear "top-basement" reflector. Blue lines are syncline axial traces. The thick dashed blue line is the "Qurm Line" (see text). (B) Base Paleocene structure contour map. The onshore map uses thicknesses from Villey et al. (1986a, 1986b) and Nolan et al. (1990) and the observed structures and dips. The major structural features are: (1) in the west, a shallow anticline, on trend with the northern plunge of the Jebel Nakhl anticline and (2) in the east, a large northwest-dipping flank extending to 7 km depth. The surface structure of the Rusayl Embayment is a north-northwest–plunging syncline that broadens toward the coast from a very tightly pinched syncline. The prominent fold on trend with northern plunge of the Jebel Nakhl anticline is pre-Late Eocene (see seismic, Fig. 8; and isopach map, Fig. 9). (C) Structural contour map of the near top-Eocene showing E-W structures formed by Oligo-Miocene and Pliocene folding. (D) Structural contour map of the near base-Pliocene, as tied to Well 3. The east-west anticline offshore (Fig. 10) is (1) at right angles to the major pre-Late Eocene anticline of Figure 6B and the anticline onshore at Mina al Fahal near Muscat; (2) high relief (2 km); and (3) intra-Pliocene.

al. (1990) described additional sections near Wadi Suq (also known as Wadi Falaj Sukh) near Sohar (700 m thick) and at Ruwaydah and Mushayq. Neither the upper nor lower stratigraphic contacts of the formation are known. The formation consists mostly of khaki-colored mudstone with decimeter beds of graded (with Bouma sequences) lithic sandstones. Conglomeratic units (up to boulder grade) include clasts of ophiolite, Hawasina chert, and Oman Exotic limestones. Toward the top are brown-colored biosparite limestones and marls. The formation is interpreted mostly as deep-water, based on the trace fossil assemblage (*Scolicia* de Quatrefages, *Palaeodictyon Meneghini* and *Spiroraphe* Fuchs), as well as the facies (Nolan et al., 1990). The formation also includes shallow-water facies in its upper part with wave ripples and an abundant and diverse, non-abraded, macrofauna. This upper part is dated, at just one locality, as Maastrichtian (at Wadi Sakin or Sakhin, near Saham, east of Sohar (Figs. 2 and 3), based on *Durania* sp., *Biradiolites* sp., *Exogyra* sp., *Lopha* sp., *Omphalocyclus macroporus (Lamarck), Orbitoides media (d'Archiac)* and *Siderolites* sp. (Nolan et al., 1990; their figure 7). No paleocurrent data have been recorded, but the formation, which contains abundant mega clasts derived from thrust sheets of ophiolite, Oman exotics, and Hawasina chert (Nolan et al., 1990), is, parsimoniously, most probably derived from erosion of uplifted areas immediately to the southeast.

These three broadly contemporaneous formations (Al Khawd, Qahlah, and Thaqab) demonstrate the presence of a post-obduction Campanian to Maastrichtian basin along the southwestern edge of the Gulf of Oman (Mann et al., 1990). The material eroded post-obduction into the onshore portion of the WGOB could include derivation from the Semail ophiolite, overlying pelagic limestones and radiolarites (Fleet and Robertson, 1980), cherts, limestones, and shales of the Hawasina complex. The Permian and younger autochthonous sequence, predominantly composed of limestones, dolomites, and quartzites of the Ordovician Amdeh Formation, were available from the Saih Hatat structure. In addition to the Amdeh Formation, potential siliciclastic input is restricted to the cherts mentioned above, detritus from the Turonian Muti Formation, and Early Jurassic Mafraq Formation, and would be expected to be modest.

Late Cretaceous: Offshore

Both Wells 1 and 3 bottomed (reached total depth [TD]) within the Late Cretaceous. Key stratigraphic control is provided by Well 3 (Figs. 4, 6, and 7). Ninkabou et al. (2021) present a graphical summary of this well (their fig. 4). The well penetrated a 3.6-km-thick section of bathyal mudstones and marls below a clear, micro-paleontologically dated, base-Paleocene disconformity at 1052 m. The oldest fossils in the pre-Paleocene section are Early Jurassic nanoplankton, thought to be reworked. In addition, the section contains abundant Middle to Early Cretaceous palynomorphs, also regarded as reworked. The oldest possibly non-reworked sample is "not younger than CC18," based on calcareous nanoplankton *Marthasterites furcatus* at 2896 m (CC18 is the lowest-but-one Campanian zone). There are, however, clear Maastrichtian forms from 1800 m (e.g., *Uniplanaris gothicus*). The section from 1052 to 4630 m (a total thickness of 3578 m) is interpreted as Campanian to Maastrichtian. It is a dark-greenish-gray or multi-colored mudstone to marl, with chert, micrite, some calcarenite, dolomitic limestones and radiolarite. There are occasional calcarenitic beds with a low quartz content (just 7%: this figure, based probably on later confidential reports, is less than suggested by the log shown in Ninkabou et al. (2021; their fig. 4). Rare layers of granule- to

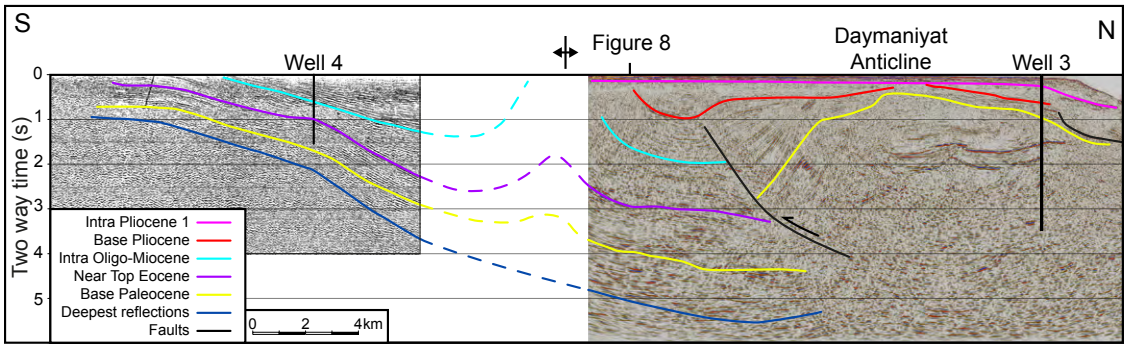

Figure 7. Composite dip section between Wells 3 and 4 (Fig. 6). Seismic data are displayed in two-way time, but note that velocities in Well 4 are significantly faster than in Well 3, meaning that in depth, the Well 4 horizons should appear relatively deeper. Well 3 (total depth [TD] 4619 m) penetrated the base-Paleogene at 1040 m and then drilled through 3600 m of Campanian to Maastrichtian deep-water marls. The base of this thick, Late Cretaceous section is not imaged. Well 4 reached TD in the Lower Eocene (Ypresian) at 2412 m. An east-west anticlinal structure in the coastal data gap between the two wells is required by the seismic mapping (Fig. 6D). The deepest mapped reflection (blue) shows a seismic character change to less coherent reflections on the onshore line (also see line drawing of seismic in Al Lazki et al., 2002) and is in accord with dip extrapolation of top-ophiolite from the surface outcrop. The nearly 600 m elevation difference in top-Paleogene between the two wells (Well 4: 1310 m vs Well 3: 752 m) requires significant uplift of the east-west (Daymaniyat) anticline post Mid-Eocene and largely pre-base Pliocene (red). Deep erosion at the intra-Pliocene unconformity (purple) is evident on this line over the crest of the Daymaniyat anticline. Earlier growth of the Daymaniyat structure was syndepositional, with rotational packages of divergent reflectors on the south flank, reflecting Eocene to Miocene rotational growth. The anticline is probably due to reversal of movement on this early fault and inversion of its hanging wall.

small-pebble conglomerate include clasts of gray dolomitic shale and quartzite. The four spot cores from this interval show dm-scale structures in the form of soft-sediment folds and small faults. Bedding in the cores is steep, up to vertical. These features suggest slumping or sliding. The depositional environment is bathyal, with neritic gastropods and bryozoans transported downslope. There are two possible interpretations of the Jurassic and older Cretaceous (i.e., pre-obduction) fossils: either they indicate allochthonous Hawasina rocks, or they represent erosion of the Hawasina sediments into a Late Cretaceous (Campanian and younger), post-obduction, deep-water basin. The latter interpretation is strongly favored and is supported by the lack of clear boundaries between the section with older fauna, the overlying Maastrichtian, and the disconformably overlying Paleocene. The more than 3.6-km-thick section of Campanian and Maastrichtian is regarded as a slope or base-of-slope sequence, comparable in facies to, and correlative with, the onshore Thaqab Formation. This conclusion is in full agreement with that of Ninkabou et al. (2021).

Paleogene: Onshore

The Paleogene rocks onshore consist of fluvial to coastal sands and conglomerates with paleosols, lagoonal deposits with minor coals, platform carbonates and deeper-water, but still shelfal, marls. The type area for the lithostratigraphy is again the Rusayl Embayment (Villey et al., 1986b; Nolan et al., 1990; Racey, 1995), where there is also good dating (Figs. 3 and 4). Paleocene fluvial and coastal conglomeratic facies are well developed in the lower half of the succession around the Saih Hatat structure (e.g., the hills east of Mina al Fahal and at Bandar Jissah; Figs. 2 and 4). They include a minor amount of ophiolitic material, together with chert, quartzite, and limestone pebbles and cobbles.

The oldest dated Paleogene in the Rusayl embayment is Late Paleocene, Thanetian (59.2 Ma–56.0 Ma: Villey et al., 1986a, 1986b; Nolan et al., 1990; Racey, 1995). There is therefore a time gap of at least 5 m.y. across the K-P Boundary. This is a regional feature across onshore Oman, with continuous sedimentation across the K-P boundary known only from two localities (Ellwood et al., 2003; Schlüter et al., 2008). Tectonic movements across the boundary have not been established in the Rusayl Embayment but are known from the Abat Basin (Fournier et al., 2006; Roger et al., 1998). Regionally, the Paleogene onlaps the Cretaceous (Nolan et al.,1990; Rabu et al.,1993). During this time, a truly dramatic change occurred. During the Late Campanian to Maastrichtian (~14 m.y.) there was deposition of at least 3.6 km and, from the seismic data, probably up to 5 km, of deep-water sediments offshore the Rusayl Embayment. After the pause in deposition across the K-P boundary in the Rusayl Embayment, some 600 m of predominantly carbonate sediments were deposited in ~18 m.y. (Late Paleocene to Middle Eocene) indicating slower subsidence. There is also less evidence of first-cycle detrital input from the ophiolite. This, together with the onlap, suggests marine transgression of a region that was no longer being actively uplifted.

Thickness changes in the Paleogene are large and indicative of active syndepositional structure formation (Fig. 4). The combined Late Paleocene to Oligocene section onshore in the Rusayl Embayment varies from 600–850 m thick (Villey et al., 1986a; Nolan et al., 1990). It also varies considerably in thickness around Muscat and is up to 1 km in the Bandar Jissah area. The larger part of that thickness variation (0 to 550 m) occurs in basal fluvial and coastal conglomeratic facies, with paleosols ("Jafnayn" facies), developed close to Saih Hatat. In the Muscat area, these conglomerate-bearing units thin markedly toward the west (from Bandar Jissah [350 m] to Ras al Hamra [20 m]). This interval is conventionally regarded as Late Paleocene, although it is only firmly dated at one place, palynologically, from a lignite interval (LeMétour et al., 1986). The 680 m of overlying limestone and marls comprise the remainder of the Jafnayn Formation, the Rusayl Formation (a Lower Eocene fluvial to lagoonal unit with conglomerates, limestones, and coals), and limestones of the Seeb Formation (Figs. 3 and 4). These last limestones are rich in fauna and dated as Thanetian to Lutetian. This coastal to inshore-marine section oversteps both the post-obduction Cretaceous and the Paleocene, to rest directly on the ophiolite (e.g., in Water Well 4; Figs. 4 and 6). There are numerous disconformities, and even local angular unconformities, within the Eocene section (within the Illerdian, Cuisian, and Lutetian; Racey, 1995). Together with the thickness variations in the basal conglomerates, they provide evidence for significant (hundreds of meters) local structural movements, on both syndepositional normal faults and folds, during Eocene deposition (LeMétour et al., 1986).

The Middle Eocene Seeb Formation at Al Khawd was interpreted by Beavington-Penney et al. (2006) as an aggradational, shallow subtidal, occasionally lagoonal, sequence. The Eocene section clearly both thickens and deepens northwest to Well 4. There, it is 1136 m thick, comprising 70–200-m-thick alternating packages of marl and limestone assigned to a bathyal to outer-neritic depositional environment, based on *inter alia,* Buliminids and dinoflagellates. The well was still in the Eocene at TD (not older than Ypresian, based on *Globigerina inaequispira*). In the Ras al Hamra area, the largely oncoidal algal biostromes are aligned north-south and faced, at least locally, sea to the west (Racz, 1979).

We therefore expect the Paleogene section to be represented on seismic data by (1) a basal planar onlap surface, possibly with minor basal erosion if the sheet-like basal conglomeratic facies were to extend offshore; (2) continuous parallel reflectors with some syndepositional subsidence variations; and (3) minor internal unconformities over individually growing structures.

Paleogene: Offshore

The offshore Paleogene was drilled in Well 3 (Fig. 7), which unfortunately is situated on an east-west–oriented growth anticline where the Paleocene section is anomalously thin (95 m). It is dark, olive-gray marl and interpreted simply as marine, with relatively scarce foraminifera. The presence of Early Paleocene is based on calcareous nanoplankton, common small *Cruciplacolithus,* and

small "*Prinsius* group." The thinning in Well 3 is a depositional thinning (condensation) rather than the result of onlap. In this well, the time gap at the K-P boundary, if present at all, is reduced compared to onshore. It was not possible for us to unambiguously correlate the base Paleocene out of this well into the grid of seismic data. We have therefore made a "jump correlation" using the onshore geology as described above, supported by dip extrapolation using the thicknesses in the Rusayl embayment. These two arguments suggest the base Paleocene surface offshore is that shown in Figure 8 and mapped in Figure 6B.

Neogene: Onshore

The uppermost Eocene recorded at outcrop is Priabonian (37.8–33.9 Ma: Racey, 1995; Rabu et al., 1993), but the sequence thins dramatically from the Lutetian upwards. The 50 m of Oligocene to Lower Miocene (*Miogypsina*) sediments (near Sultan Qaboos University) are heterogeneous: marls, limestones, and rudites including abundant reworked Middle Eocene material. Well 4 encountered up to 230 m of middle- to outer-neritic Oligocene (*Globigerina tripartita, Globigerina selli, G. gortanii,* and *G. angiporoides).* Offshore Well 3 (Fig. 7) shows a thinned section between the Middle Eocene and the Miocene (~160 m). A broad pattern of shallowing and a break or condensation between Late Eocene, Priabonian, and Miocene is evident onshore. The precise acme of this hiatus in terms of structuration is unfortunately poorly constrained.

In the area near Sultan Qaboos University and 1 km east of Wadi Rusayl, there are ridges of reef limestone of Late Oligocene to Miocene age resting on conglomerates. PDO water well (WW) 9 encountered 601 m of Pliocene to Quaternary pebbly sands without finding their base (Fig. 6D).

Neogene: Offshore

Lower Miocene reefal carbonates outcrop on the Daymaniyat islands off Barka and at Sawadi, but the Miocene is barely known from surface exposures onshore. Well 4, however, drilled 1200 m of post-Eocene, broadly upward-shallowing, outer neritic and shallower, marls, sands and conglomerates. Well 3, drilled on the crest of an anticline, encountered just 200 m of Miocene and Pliocene carbonates (Fig. 7). The thinness of the Neogene in Well 3 and the growth fault to the south of the well (Fig. 7) both pose problems in correlating the deeper Neogene away from this well. However, there is a good tie to the "near-base Pliocene." Dip extrapolation from the Late Eocene outcrop and the thickness of Pliocene encountered in WW 9 are both consistent with the mapped structure of the red marker offshore, as shown in Figure 6D, which is therefore interpreted as near base Pliocene.

Structural Timing

The correlation of Wells 3 and 4 with the seismic data is shown in Figure 7. As described above, Well 3 (TD 4630 m) drilled 3600 m of Campanian to Maastrichtian deep-water marls with debris flows. The top-ophiolite reflector, which is shown by clear seismic character changes onshore (Al Lazki et al.,

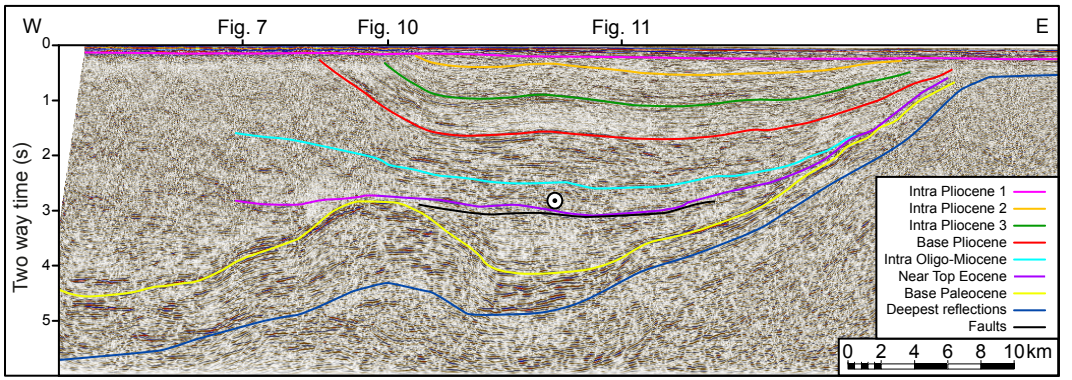

Figure 8. This coast-parallel (Fig. 6) seismic line shows a major onlap surface (purple) that is correlated with the base-Paleogene (K-P) unconformity. The blue horizon is the deepest mapped set of reflections and is interpreted as "near Base Cretaceous" (see text). The buried pre-late Eocene anticline (center left) has a north-northeast–south-southwest axis and is on trend with the Jebel Nakhl structure (Fig. 6A). The "near Top Eocene" (magenta) horizons are tied indirectly to Well 4. The gently dipping fault above the base-Paleogene is a strike section through the décollement beneath the Pliocene-age east-west anticline (Fig. 6D). This anticline is shown best in dip section in Figure 10. The near-base Pliocene and intra-Pliocene 1 horizon (red and purple, respectively) can be correlated into Well 3.

2002), is apparently not imaged on the offshore line. The base of the Late Cretaceous section in Well 3 is also not imaged (Fig.7). Well 4 reached TD in the Early Eocene (Ypresian) at 2448 m. As argued above, interpretation of "base Paleocene" away from the wells is based on (1) the expected seismic character, with a better imaging of continuous parallel reflectors in the Paleogene limestones and marls than the underlying Late Cretaceous marls; and (2) correlation around the seismic grid of the onlap surface. The change in Eocene thicknesses between the wells demonstrates syndepositional growth of the east-west–trending Daymaniyat anticline structure as a roll-over structure to a Late Eocene extensional growth fault. The anticline was clearly also tightened tectonically by compression during the Oligo-Miocene. The Late Eocene marker divides the growth of the anticline into wedges of reflectors on the northern flank of the structure. The final mild folding is, however, intra-Pliocene, because the near-base Pliocene horizon is gently folded (Fig. 7). In summary, we interpret the north-dipping fault as first acting as an Eocene growth fault and subsequently as a Miocene and younger reverse fault.

The coast-parallel seismic line (Fig. 8) shows, in its eastern half, the distinctive major onlap surface interpreted as base Paleogene. Below this, the blue horizon, the deepest mappable surface, is interpreted as near base-Cretaceous. We do not know what the reflectivity change at this level represents. It lacks both the diffractions that might be associated with top-ophiolite and a strong hard reflector that would be expected at the top of the seismically fast autochthonous carbonate sequence. The deep syndepositional anticline suggested by thinning of the Paleocene–Eocene (center left on Fig. 8) has a north-northeast–south-southwest axis and is down-plunge from the Jebel Nakhl structure. The isopach map (Fig. 9) shows its structural amplitude, which was Paleocene–Eocene only. Well 4 not only encountered a thicker Paleocene–Eocene sequence than at Rusayl (1186 m [base not seen] versus 850 m) but also outer neritic facies in the Eocene, contrasting with shallow-subtidal, lagoonal facies at both Al Khawd and Rusayl. The general regional thickness increase toward the west is therefore also toward deeper-water, more basinal conditions at this time. The long base-Paleogene flank from 7 km to 1 km depth to the east in the offshore (Figs. 6B and 8) could be viewed as a continuation of the onshore northwest-dipping flank of the Saih Hatat dome. This offshore flank continued to rotate until the Pliocene, with no evidence of tectonic pulses.

The major offshore anticline axes (red lines on Fig. 6) show growth during the Pliocene. They were uplifted and peneplaned during the late Pliocene (e.g., Fig. 10), even though some, such as the East-West Daymaniyat anticline (Figs. 7 and 11), also have Eocene growth histories. The major Late Pliocene planar angular unconformity, seen over the entire offshore portion of the study area

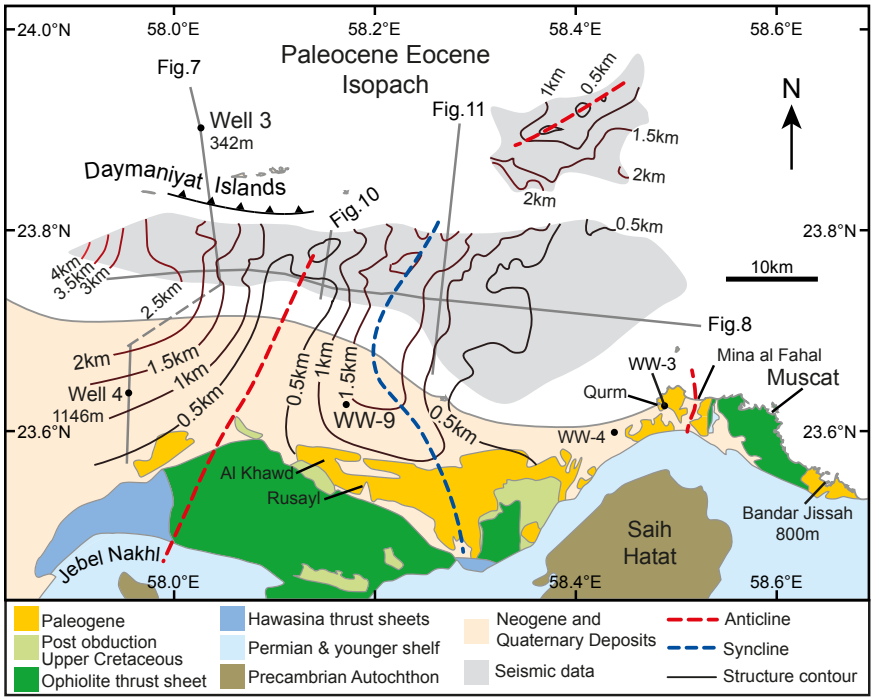

Figure 9. Isopach map of the Paleocene–Eocene sequence. The map is incomplete to the north due to difficulty correlating across the Pliocene Daymaniyat anticline. The thickness changes show growth of a north-south fold structure on trend with the Jebel Nakhl anticline and onlap onto the rotating eastern flank of the offshore Rusayl Embayment.

(Figs. 8 and 10), shows erosion of several kilometers of sediment from the crests of major box-fold anticlines.

Comparison with Onshore Structural Timing

Apatite fission-track (AFT) age data (Poupeau et al., 1998) were interpreted as showing that Saih Hatat rocks cooled below 60° from 53 Ma (Early Eocene; Ypresian) onward, and that their temperatures subsequently remained stable. Saddiqi et al. (2006) optimized this analysis with path-length modeling, suggesting an earlier (58 Ma, Thanetian, Late Paleocene) end of the period of rapid cooling. However, Hansman et al. (2017) re-evaluated all the previous zircon fission-track and AFT data and added new data from both Jebel Akhdar and Saih Hatat. They concluded that major uplift of Saih Hatat occurred at the latest by 70 Ma (Maastrichtian) and ended between 60 Ma and 50 Ma (Paleocene to Early Eocene). Uplift of Jebel Akhdar is less well constrained with a lesser amount of uplift and cooling than Saih Hatat in this period. Between 50 and 40 Ma (Mid-Eocene), no major uplift and cooling occurred. A second phase of uplift and cooling is interpreted between 40 Ma and 30 Ma (Late Eocene and Oligocene) with uplift of Jebel Akhdar being greater (three times more cooling than Saih Hatat) during this second phase. These conclusions are in good accord with the onshore depositional history and sedimentology described above.

Offshore, the Late Eocene to Oligocene period is one of continuing growth of anticlines related to syndepositional growth faults (Fig. 7). This section is thin (Fig. 4) in both Wells 1 and 3, both drilled on anticlines. The section is faulted out in Well 2. In general, the interval from Late Eocene to Oligocene appears to be one of relatively less sediment input to the hinterland basin than either the Late Cretaceous or the Mio-Pliocene, as also reported by Ravaut et al. (1997) and Ninkabou et al. (2021). Factors such as climate and lithology play a role, as well as simple uplift in determining sediment budgets. But it is possible that low sediment input during a time of active uplift was in part because the sediments being eroded onshore at this time were in large measure the youngest overburden, shallowly buried Paleogene carbonates. Hence this resulted in dissolved, rather than solid sediment, in the basin fill (Allen, 2017).

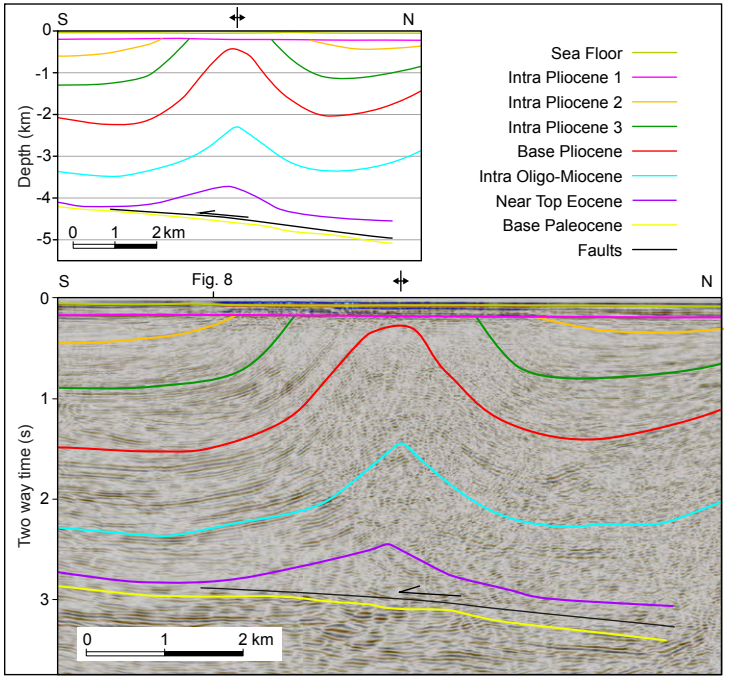

Figure 10. Dip section through a major east-west anticline (Fig. 6). The line drawing has no vertical exaggeration. This angular fold affects sediment as young as Mio-Pliocene and is truncated by a spectacular planar unconformity dated as intra-Pliocene in the Well 3 (Fig. 7). The lack of onlap or wedging indicates that the fold was formed in a short-lived folding event. This is in contrast to the near-parallel and older (Oligo-Miocene) Daymaniyat fold, which is clearly syndepositional (Fig. 7). The fold style, which is the same as that affecting Paleogene sediments onshore, requires a décollement above the Late Cretaceous sediments. The most likely décollement horizons on the basis of the onshore geology are the Rusayl Formation (Ypresian) or the base Cretaceous. The age interpretations of the horizons presented here are consistent with a décollement in the Rusayl Formation. An additional dip section across this fold is shown down-plunge to the east in Figure11. It is also seen in strike view in Figure 8.

BATINAH COAST AND ADJACENT OFFSHORE

Onshore

Along the Batinah plain (Fig. 12), the gravity data were interpreted to indicate a planar seaward-dipping top to the ophiolite mass (Shelton, 1990). Mann et al. (1990, p. 553) describe an extensional arcuate fault separating Upper Cretaceous and Paleogene "cover rocks" from their basement of the Semail and Hawasina thrust sheets: the "Batinah Coastal fault" (Fig. 12B; Mattern and Scharf, 2018). In places along this fault, Mann et al. (1990) were able to document a series of low-angle, down-to-the-basin extensional faults to the northeast of this boundary and within the Cretaceous and Paleogene sediments. Roll-over anticlines occur in the hanging wall of some of these faults (e.g., at Mushayq). The faults were therefore interpreted to be listric. The Late Campanian to Maastrichtian Thaqab Formation on the Batinah plain was discussed above.

Offshore

Available offshore seismic data show no clear top-basement reflection. The reflection energy and continuity dies out downwards. There is, however,

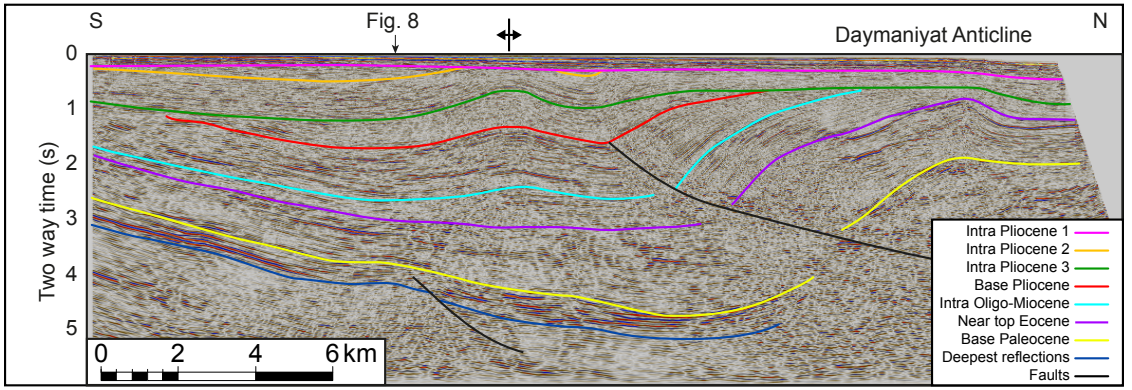

Figure 11. North-south seismic line through the Daymaniyat anticline and the eastern extension of the anticline of Figure 9, showing the contrasting styles of the largely syndepositional Eocene and younger Daymaniyat structure and the postdepositional Pliocene-age structure.

a package of two or three relatively strong reflections. These reflections typically occur between four and five seconds, dipping seaward, on the extreme inboard (southwest) end of the seismic lines, and they tie from line to line, terminating northeast along the boundary shown in green on Figure 12A. This termination is interpreted as the footwall cut-off of a deeply buried down-to-the-basin extensional fault running parallel to the coast. Based on a regional dip extrapolation from onshore and the gravity work of Shelton (1990), the termination of this reflective sequence appears to mark an extensional fault close to the top of the ophiolite. Offshore, we unfortunately have no direct evidence for the depth to top-basement. Ninkabou et al. (2021) interpret a top-basement near the horizon we refer to as "deepest reflections." We interpret this as near-base Campanian, based on the well ties to Wells 1 and 3. Our caution in calling this "top-basement" is based on the following: (1) The view that a reasonable seismic velocity contrast is to be expected at the boundary of likely overpressured Cenomanian to Maastrichtian mudstones and any form of basement; and (2) that there is, consequently, uncertainty whether lack of seismic imaging or lack of reflection energy is the cause for the change in reflectivity. Their "top basement" and our "deepest reflector" horizons are very close to the TD of Well 3. The difference is subtle, and in our view, there could be more Campanian sediment below the TD of this well. A top-basement near this level makes a lot of geological sense and would agree with the gravity modeling of Ravaut et al. (1997, 1998).

The WGOB can be divided into northern, central (Fig. 13), and southern (Fig. 14) areas. In the northern and southern areas, Wells 1 and 3, respectively, demonstrate a thick Late Cretaceous basin fill, which is correlated, both in age and facies, with the Thaqab Formation. In the central area, Well 2 documented a thick Mio-Pliocene section associated with a major down-to-the-northeast extensional gravitational fault (Figs. 12B and 12C).

In the north, Well 1 (Fig. 4) proved Late Campanian age sediments at TD. The most precise age determination is based, as in Well 3, on *Marthasterites furcatus* (CC18), but a Campanian age is also supported by foraminifera *Globigerinita elevata* and consistent occurrence of *Globotruncana struati* at 3232 m. Reworked Late Cretaceous biota were also found in the Campanian section. The depositional environment of the Campanian to Maastrichtian is bathyal, based on planktonic foraminifera. This section, 755 m thick in Well 1, is predominantly claystone, a varicolored, brown, light-green, or gray-green claystone with rare clasts of limestone and siltstone. The Campanian section has variable amounts of limestone and more marl with a thin interval of wackestone to packstone. The thick Campanian to Maastrichtian seen in Well 3 in the south can be followed offshore (Fig. 14). The deepest mapped reflection package at the southern end of this line is at ~5 s two-way travel time (TWT). Simple extrapolation to the northeast would suggest a minimum pre-Paleocene sediment thickness of 5 km at the well location.

Seismic data show that Wells 1 and 3 both penetrated a conformable Paleocene–Cretaceous contact. The Paleocene sections are both thin (Well 1: 105 m; Well 3: 95 m). They also both show a thinned section between the Middle Eocene and the Miocene (~160 m and 185 m, respectively), reflecting local syndepositional structural growth of their respective anticlines. In the central area of the WGOB (Fig. 13) , Well 2 shows more than 3 km thickness of Miocene and 640 m thickness of Pliocene. Both sections are sandy and conglomeratic (with clast size up to 20 cm), including ophiolitic debris, cherts, and limestones with interbedded gray to brown shale. In a zone 20 km wide, along the coast, the seismic data reveal a set of two or three down-to-the-basin, listric, normal faults, each with roll-over anticlines (axes indicated in red on Figs. 12B and 12C) in a complex belt of ~10 km wide, en-echelon, fault-bounded structures. Well 2 was drilled mostly in the hanging wall of one of these growth faults, which accounts for the 3640-m-thick Neogene section. It was drilled through a fault into the footwall just above TD (it is shown projected into a similar position in Fig. 13). The bottom core taken in this footwall section had vertical bedding, Cretaceous (not older than Turonian) microfossils (unspecified). These sets of offshore growth faults are the offshore extension of the low-angle extensional faults documented by Mann et al. (1990) onshore.

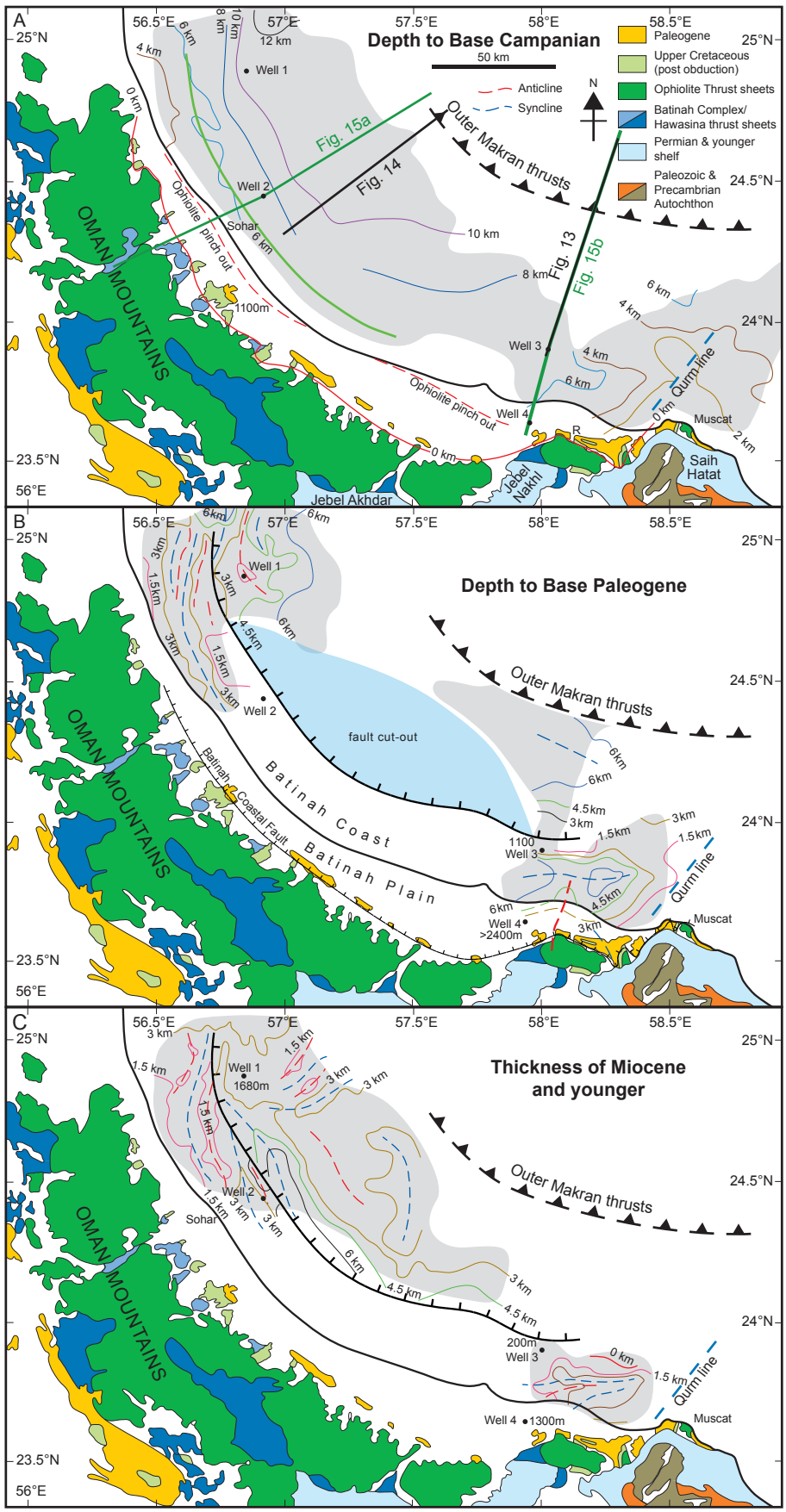

Figure 12. (***Continued on following page.***)

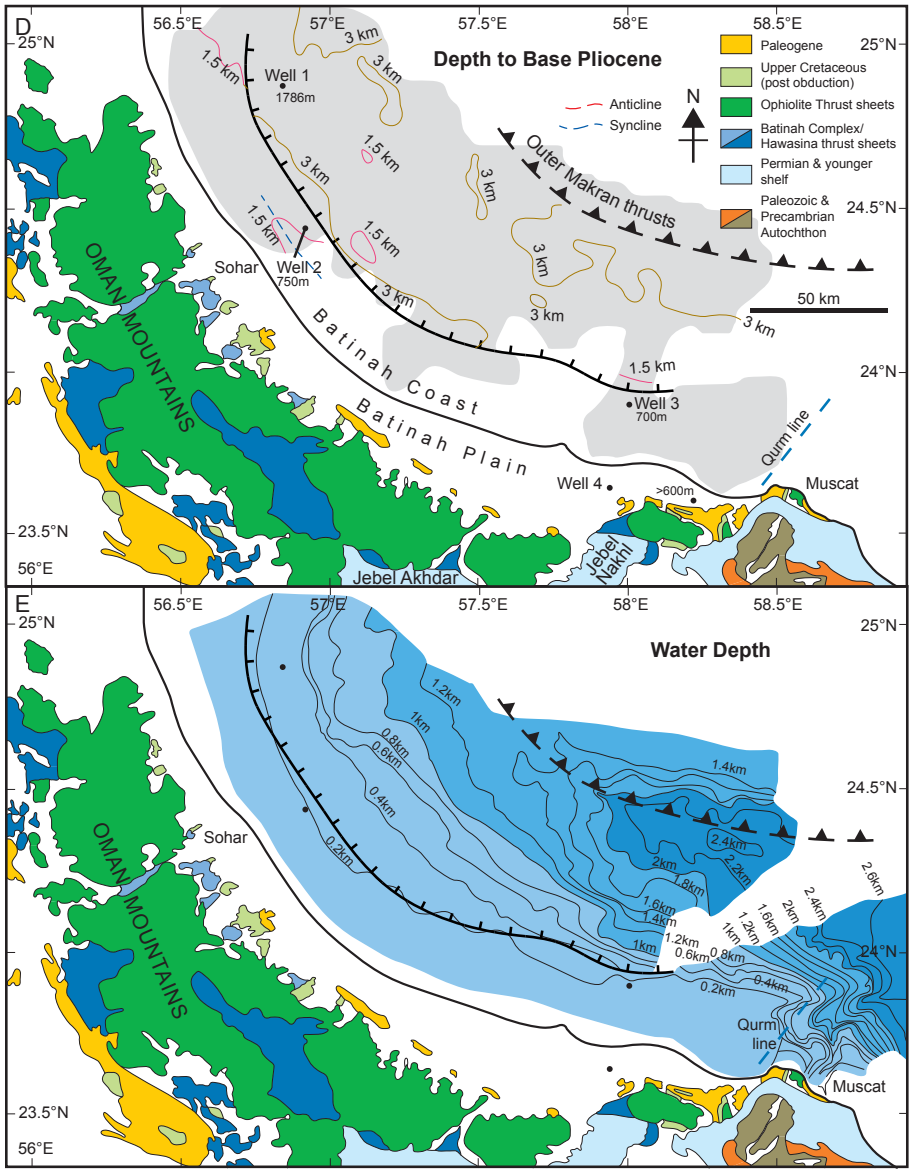

Figure 12 (*continued*). Maps of Batinah study area. The gray areas are the extent of the seismic data that were interpreted and mapped for each of the horizons. (A) Structure contours (contour interval 2 km) on deepest seismic reflections interpreted as near-base Campanians. The zero isopach line onshore is the structural base of the post-ophiolite section; this contact is normally faulted (Mann et al. 1990). Seismic coverage is indicated by the gray shading. The solid red line is the zero sediment-thickness isopach (current outcrop edge). The dashed red line is the 0 mgal residual Bouguer anomaly from Shelton (1990), which is close to his inferred ophiolite pinch-out line for a flat-based ophiolite slab. The green line represents the seaward termination of a set of seaward-dipping reflectors that are in dip conformity with the top ophiolite. Beyond this line, there is no clear base reflection to the sedimentary sequence on the seismic data (which was recorded to 8 s two-way travel time [TWT]). All these features parallel the gravity-modeled dip of the upper surface of the ophiolite. It is suggested that they are all driven by the top-ophiolite dip surface, which has set up a basin margin for the Western Gulf of Oman Basin (WGOB) Hinterland basin. Offshore seismic lines are shown in Figures 13 and 14. Sketch cross sections are shown in Figures 15A and 15B. (B) Structure contours of base Paleogene (contour interval 1.5 km). The onshore Batinah Coastal faults (Mann et al., 1990; Mattern and Scharf, 2018) are a set of low-angle extensional faults down-throwing northeast. The solid black line marks the extent of a major extensional gravitational fault (Fig. 14). The light blue shaded area is the extent of the fault cutout at intra-Miocene (?) level; a minimum for lateral displacement at deeper levels. Between this fault and the coast is a domain of smaller, listric, syndepositional normal faults affecting both Late Cretaceous and Cenozoic sediments. Axes of the associated set of rollover anticlines axes are indicated in red. (C) Thickness of Miocene and younger (contour interval 1.5 km). Note the depocenter in the center of the study area. This is basin fill (4) in Figure 3. (D) Structural contours on base Pliocene (contour interval 1.5 km). (E) Modern sea floor bathymetry (contour interval 200 m) from seismic data. Note the change between the smooth depositional sea floor west of Qurm, and the erosional gullied margin developed on the extension of the Muscat ophiolite to the east. The white re-entrant without data is due to absence of seismic coverage.

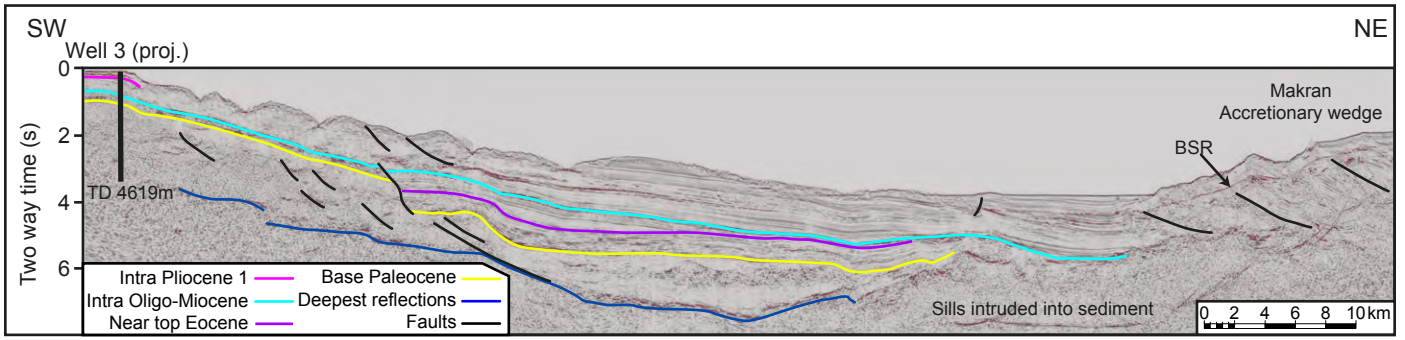

Figure 13. The Late Cretaceous "Hinterland" Basin of the Western Gulf of Oman. The dark-blue horizon (left) marks "deepest reflections" and is mapped in Figure 12A as near-base Campanian. The Upper Cretaceous alone could exceed 5 km in thickness on this line. Well 3 penetrated 3.6 km of this interval. Curved concave-up acoustically hard reflectors near the northeast end of the line are mappable across a grid of lines and are interpreted as igneous sills, possibly of Eocene age, if related to onshore intrusions discussed in (dated by) Scharf et al. (2020). In this southern portion of the Western Gulf of Oman Basin (WGOB), the post-Oligocene fill is less in thickness than the central portions (Fig. 14). For line location, see Figure 12A. A nearby line (their Line A) was published by Ninkabou et al. (2021). BSR—Bottom simulating reflector, an indication of the base of gas-hydrate–bearing sediment.

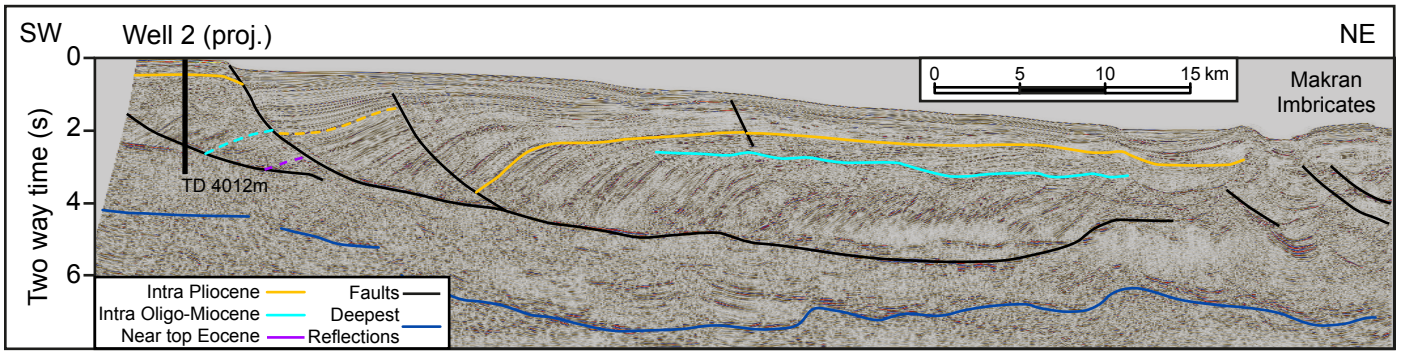

Figure 14. The Mio-Pliocene fill of the central Western Gulf of Oman Basin (WGOB). In Well 2, 3560 m of Miocene and 640 m of Pliocene marls, sands, and conglomerates were drilled (here projected 20 km along strike from the northwest into an equivalent structural position). A set of three major listric growth faults has transported neritic deposits into the deep water by rotational sliding on the clays of the Upper Cretaceous. The landward equivalent of these was encountered near total depth (TD) in the well (4012 m). Several angular unconformities occur in the hanging wall block of the seaward fault, the deeper of which (cyan) is the more laterally extensive. It is possible that this is the "regional" Upper Miocene unconformity of the literature, which is a hiatus in Wells 1 and 2, and offshore Fujairah (Jung and Ali, 2018). This would imply that the light brown event is the intra-Pliocene unconformity, also seen in this study above major structures around the Daymaniyat islands. However, none of the surfaces on this line can be directly dated by correlation to the wells. The largest normal fault breaks the sea bed, illustrating active faulting at the shelf edge to the present day. The area of fault cut-out estimated at Paleogene level and the line location are shown in Figure 12A.

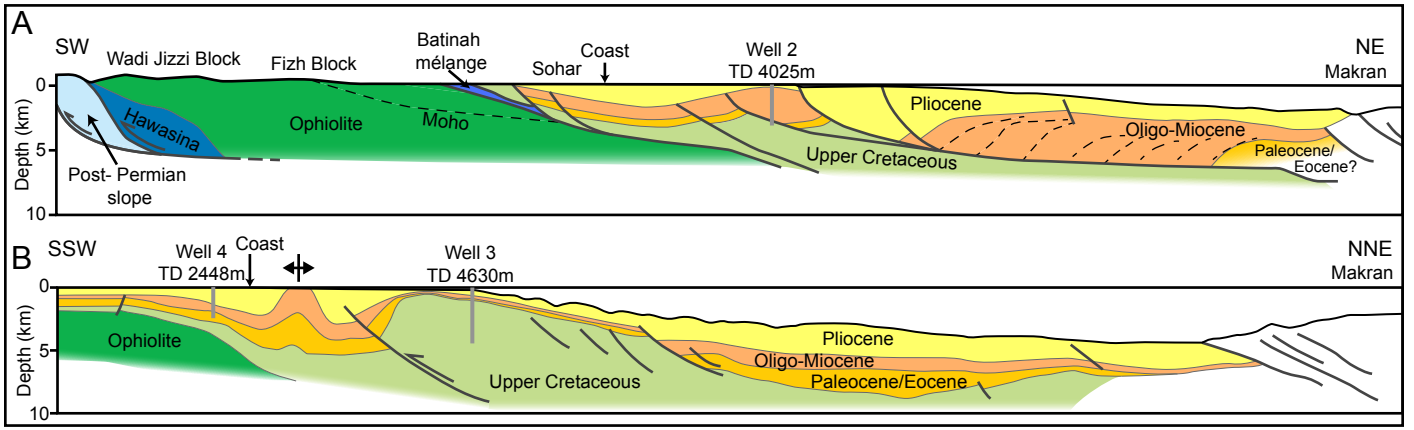

Figure 15. Sketch synoptic sections through the Western Gulf of Oman basin. (Line locations in Figures 2 and 12A). Onshore geology in (A) is simplified from Lippard et al. (1986) and the shape of the ophiolite bodies is from Shelton (1990). (A) Offshore Sohar: shows the relationship between the top-ophiolite, the Batinah Coastal faults, and a set of inboard smaller growth faults that are inferred to have formed along the seaward-sloping top surface of the ophiolite in the Late Cretaceous. This geometry controlled Late Cretaceous deposition in the deep-water Western Gulf of Oman Basin (WGOB) and its onshore equivalent: the Thaqab Formation. (B) This section combines Figures 7 and 13 into a single profile. Note that compressional deformation is associated with the coastal zone of the WGOB, where the sediments abut against the dipping upper surface or faulted footwall of the ophiolite.

The central part of the basin is dominated by a single rotational gravitational growth fault with a 50-km-long, subhorizontal section of fault plane in dip section (Figs. 12C and 14). This northwest-southeast fault has a length along strike of 150 km with tip lines 50 km north of Sohar and just northwest of Well 3. In the southeast, the tip line is simple, but to the northwest, the total displacement dies away via a set of smaller and steeper syndepositional extensional faults with north-south strikes. Our best estimate is that this fault was active from at least the Eocene (probably older) to the present day (Fig. 14; note the modern sea floor offset). An angular unconformity above the inboard portion of the rotated strata in the growth-faulted section is dated as intra-Pliocene in Well 2. Extension on this major fault is uncompensated by toe-thrusting in the center of the basin; however, toward the tip lines of the system, both to the northwest and to the southeast, there is partial compensation of extension by sets of toe thrusts.

Inboard of this major growth fault in the southern WGOB is another post-Eocene depocenter, with up to 4500 m of post-Eocene, mostly Mio-Pliocene neritic sands, conglomerates, and limestones being deposited within 20 km of the coast. Thickening toward this depocenter is seen on the western end of Figure 8. Well 4 proved at least 1300 m of this thickness. Data are not available to map the northwestward extent of this depocenter.

Sediment supply from the Oman Mountains and subsidence of the WGOB were both renewed in the Early Miocene. Deposition of up to 4–5 km of sediment offshore in the WGOB was interrupted only by a Late Miocene disconformity or condensed zone, but was resumed in the Pliocene. The intra-Miocene disconformity on growing structures is evident biostratigraphically in both Wells 1 and 3. The hiatus is dated as Late Miocene–Tortonian (between nanoplankton zones NN6 and 11). However, in neither Wells 1 nor 3 is there clear evidence of an unconformable contact at this level.

Figures 12, 13, and 14 illustrate the Late Cretaceous and Mio-Pliocene depocenters. The following sub-parallel features occur between the basement outcrops and the depocenters of the WGOB (Figs. 12A and 12B). (1) The onshore Batinah Coastal faults (Mann et al., 1990) are interpreted as low-angle extensional faults within the Late Cretaceous and/or Cenozoic rocks (Fig. 12B). (2) The 0 mgal residual Bouguer anomaly from Shelton (1990) is close to his inferred ophiolite pinch-out line for a flat-based ophiolite slab (red dashed line on Fig. 12A). (3) The seaward termination of a set of seaward-dipping reflectors is in dip-conformity with the top ophiolite (green line on Fig. 12A). (4) Offshore again, and parallel to all of the above, the large, low-angle Cenozoic gravitational extensional fault dominates the center of the study area (Figs. 12B and 14). All these features parallel the modeled strike of the upper surface of the ophiolite based on gravity data (Shelton, 1990). It is suggested that they are all driven by the top-ophiolite dip surface, which has set up a basin margin for the WGOB. The simplest synthesis consistent with the geophysical and geological data presented is that of a top-ophiolite surface that dips toward the NE at 12°–30°. Given the wedge shape of the ophiolite, modeled from gravity data (Shelton, 1990), this dipping surface at the top of the ophiolite could well itself be a low-angle extensional fault, down-throwing the oceanic crust into the Western Gulf of Oman and separating obducted

ophiolite to the southwest from in situ oceanic crust of the Gulf of Oman to the northeast.

DISCUSSION AND CONCLUSIONS

Combining stratigraphy (onshore geology and offshore wells) and structure (onshore geological mapping and offshore seismic interpretation) has revealed more details of the tectonic evolution of the Oman Mountains and their relationship to the offshore geology. We interpret Paleocene to Late Eocene growth of tens of km wavelength fold structure in the offshore extension of the current Jebel Nakhl fold axis (Figs. 8 and 9). This folding is coincident in timing with uplift and cooling recorded in both Saih Hatat and, less strongly, in the Jebel Akhdar structures (Hansman et al., 2017).

Syndepositional, low-amplitude, north-south folds and east-west growth faults offshore the Rusayl Embayment resulted in thickness differences of shallow-water sediments throughout the Paleocene and Eocene (Fig. 9). Rollover anticlines associated with the east-west growth faults were inverted and thrusted during the Neogene (e.g., Figs. 7 and 11). Oligo-Miocene through Pliocene tightening of preexisting folds resulted in severe thinning over anticlines (for example, the hanging-wall anticline over the south-verging reversed normal fault underlying the Daymaniyat Islands anticline; Fig. 7). Seismic mapping demonstrates that compressional structures are aligned with the trailing edge of the ophiolite, (i.e., east-west in the Rusayl Embayment (Fig. 6D) and northwest-southeast off Sohar (Fig. 12B). A major phase of compressional shortening occurred within the Pliocene (Figs. 10 and 11). These structures have a dominant box-fold geometry and east-west fold axes. Major planation of these structures occurred in the late Pliocene.

In terms of shortening directions, we see evidence of east-west compression in the Late Eocene (Figs. 8 and 9) and north-south compression in the Oligo-Miocene through Pliocene (Fig. 6D). Major box folds with north-northwest–south-southeast fold axes affecting Paleocene–Eocene limestones above the ophiolite onshore between Ras al Hamra and Bandar Jissah could be related to the pre-Late Eocene east-west compression phase.

The "Western Gulf of Oman Basin" has two major phases of sedimentary fill (each at least 3–4 km), one in the Late Cretaceous, and one during the Mio-Pliocene. The Late Cretaceous phase is coeval with the younger part of the fill of the Aruma (Fiqa) foreland basin southwest of the Oman mountain belt. The second phase of subsidence may be a response to a second episode of crustal shortening and folding throughout the Neogene.

Along the smoothly curving Batinah coast, there is parallelism between a major low-angle normal fault system separating the Cretaceous and Eocene onshore, the strike direction of the top-ophiolite surface, based on the few onshore seismic lines reported in the literature (Shelton, 1990; Al Lazki et al., 2002), the gravity anomaly marking the northeastern termination of the ophiolite nappes, and a seismic-reflection boundary at the extrapolated position of near-top-ophiolite. To the northeast in the Gulf of Oman, a 150-km-long system of growth faults culminates in an enormous 60-km-long, gravity-driven slide along a seismically imaged, low-angle extensional fault. An interpretation of all these features, which is consistent with the gravity modeling of Shelton (1990) and Ravaut et al. (1997, 1998), is that the boundary between the obducted ophiolite and Gulf of Oman oceanic crust top surface is a low-angle extensional fault dipping seaward at 12°–30°, cutting out the ophiolite completely very close to the present coast and juxtaposing sub-ophiolite rocks with, probably oceanic, Gulf of Oman crust.

Along strike to the southeast, all these linear features and both the Late Cretaceous and Mio-Pliocene basins themselves, are terminated at the "Qurm Line," along the northward offshore projection of the "Saih Hatat promontory" (Ninkabou et al., 2021). The Qurm Line is so-named because of the obvious topographic contrast related to the above between the wide sweeping bay of the Batinah coast and the rocky headlands at Qurm and to the east. Ninkabou et al. (2021) regard this line as a manifestation of the east side of the Semail fault zone. However, the Semail Gap fault terminates at the northern limit of the Semail Gap and does not cut across the shelf carbonates. The major anticline fold axis of Jebel Akhdar (aligned west-northwest–east-southeast) swings around 90° into alignment with the north-northeast–south-southwest–aligned Jebel Nakhl anticline, which then swings around through 90° to align west-northwest–east-southeast along the Fanjah saddle to Saih Hatat (Searle, 2007; his figure 17). There is no offset of the Semail Gap along the Fanjah saddle; so this structure must be a Late Cretaceous ophiolite obduction-related lateral ramp and not a later Cenozoic feature. The Rusayl Embayment is a large accommodation structure caused by the transition from the deep hinterland basin in the northwest and an uplifted subduction–high-pressure metamorphic complex in the southeast.

A major low-angle normal fault dominates the central portion of the WGOB (Figs. 12B and 14). It has caused enormous stratigraphic expansion of the Eocene–Recent section in the central portion of the WGOB and remains an active sea floor fault. It is similar in geometry to the Vicksburg detachment in the Gulf of Mexico (Whitbread et al., 2001). During the entire formation of this fault, the Arabian plate has been approaching the Makran subduction zone (Platt et al., 1985), the current rate, measured by GPS as 2 cm a^{-1} (Vigny et al., 2006). At this rate of motion, 680 km of convergence is estimated since the end of the Eocene. However due to the off-scraping of sediment, the 400-km-wide Makran accretionary wedge has also been accreting seaward, recently at 1 cm a^{-1} (White, 1982; Platt et al., 1985). On the basis of these current rates, the 60-km-long hanging wall of this fault was slipping into abyssal depths for much of its history and has only recently impinged on the front of the Makran accretionary prism.

Sediment isopachs from offshore seismic data show that there is no evidence for the proposed "Muscat-Musandam high" of Ravaut et al. (1998) and Breton et al. (2004). The clear gravity anomaly must have another explanation, such as a basement density difference or an over-corrected gravity field in areas of significant but poorly constrained bathymetry. Hence, the "Sohar Basin," at least as defined by Ravaut et al. (1997, 1998), is simply part of a larger Western Gulf of Oman Basin.

ACKNOWLEDGMENTS

We are grateful to the Ministry of Oil and Gas, especially Dr. Salman al Shidi, for making available the seismic and well data from offshore Oman and approving publication of this work. Petroleum Development (Oman) Ltd. and current and former employees of PDO, especially Craig Harvey, Nick Feast, Mark Hollanders, and Jan Schreurs are thanked for their exceptional cooperation and assistance. We thank Caroline Haworth for her work interpreting offshore seismic data. Numerous geologists from a variety of companies have contributed expertise and insights, as usual mostly anonymously, to the confidential well reports kindly made available to us by the Ministry of Oil and Gas in Oman, and these contributions are gratefully acknowledged.

We also thank Owen Green for his help in the field and with paleontology and Mohammed Ali, Tony Watts, and Brook Keats for ongoing discussions and constructive reviews of the manuscript. We thank Martino Foschi for managing the seismic data and Alastair Robertson and an anonymous referee for detailed and constructive review of the manuscript, which has improved it immensely.

REFERENCES CITED

Abbasi, I.A., Hersi, S.O., and Al-Harthy, A., 2014, Late Cretaceous conglomerates of the Qahlah Formation, north Oman, *in* Rollinson, H.R., Searle, M.P., Abbasi, I.A., Al-Lazki, A., and Al Kindi, M.H., eds., Tectonic Evolution of the Oman Mountains: Geological Society of London Special Publication 392, p. 325–341, https://doi.org/10.1144/SP392.17.

Al Anboori, S., 2004, Exploration opportunities in Oman - Block 18. Al Hajar Quarterly Newsletter of the Geological Society of Oman March 2004, p. 3, http://www.gso-oman.org/publications/al-hajar/.

Ali, M.Y., and Watts, A.B., 2009, Subsidence history, gravity anomalies and flexure of the United Arab Emirates (UAE) foreland basin: GeoArabia, v. 14, no. 2, p. 17–44.

Ali, M.Y., Watts, A.B., and Searle, M.P., 2013, Seismic stratigraphy and subsidence history of the United Arab Emirates (UAE) rifted margin and overlying foreland basins, *in* Hosani, K.A., Roure, F., Ellison, R., and Lokier, S., eds., Lithosphere Dynamics and Sedimentary Basins: The Arabian Plate and Analogues: Berlin, Heidelberg, Springer-Verlag, p. 127–143, https://doi.org/10.1007/978-3-642-30609-9_6.

Ali, M.Y., Watts, A. B., Searle, M. P., Keats, B., Pilia1, S., and Ambrose, T., 2020, Geophysical imaging of ophiolite structure in the United Arab Emirates: Nature Communications, v. 11, https://doi.org/10.1038/s41467-020-16521-0.

Al-Lazki, A.I., Seber, D., and Sandvol, E., 2002, A crustal transect across the Oman Mountains on the eastern margin of Arabia: GeoArabia, v. 7, no. 1, p. 47–78.

Allen, P.A., 2017, Sediment Routing Systems: The Fate of Sediment from Source to Sink: Cambridge University Press, 407 p, https://doi.org/10.1017/9781316135754.

Beavington-Penney, I., Wright, V.P., and Racey, A., 2006, The Middle Eocene Seeb Formation of Oman: An investigation of acyclicity, stratigraphic completeness, and accumulation rates in shallow marine carbonate settings: Journal of Sedimentary Research, v. 76, p. 1137–1161, https://doi.org/10.2110/jsr.2006.109.

Boote, D.R.D., Mou, D., and Waite, R.I., 1990, Structural evolution of the Suneinah foreland, Central Oman Mountains, *in* Robertson, A.H.F., Searle, M.P., and Ries, A.C., eds., The Geology and Tectonics of the Oman Region: Geological Society of London Special Publication 49, p. 397–418., https://doi.org/10.1144/GSL.SP.1992.049.01.25

Breton, J.-P., Béchennec, F., Le Métour, J., Moen-Maurel, L., and Razin, P., 2004, Eoalpine (Cretaceous) evolution of the Oman Tethyan continental margin: Insights from structural field study in Jabal Akhdar (Oman Mountains): GeoArabia, v. 9, no. 2, p. 41–58.

Calvache, J., and Love, C., 2001, New geological findings in the Gulf of Oman (Northern Sohar Basin) Shell Oman Deepwater Block 18: Abstract, International Conference on the Geology of Oman, Sultan Qaboos University, Muscat: GeoArabia, v. 6.2, p. 292–295.

Coffield, D.Q., 1990, Structures associated with nappe emplacement and culmination collapse in the Central Oman Mountains, *in* Robertson, A.H.F., Ries, M.P., and Ries, A.C., eds., The Geology and Tectonics of the Oman Region: Geological Society of London Special Publication 49, p. 447–458, https://doi.org/10.1144/GSL.SP.1992.049.01.28.

Cooper, D.J.W., 1988, Structure and sequence of thrusting in deep-water sediments during ophiolite emplacement in the south-central Oman Mountains: Journal of Structural Geology, v. 10, p. 473–485, https://doi.org/10.1016/0191-8141(88)90035-1.

Ellwood, B.B., MacDonald, W.D., Wheeler, C., and Benoist, S.L., 2003, The KT boundary in Oman: Identified using magnetic susceptibility field measurements with geochemical confirmation: Earth and Planetary Science Letters, v. 206, p. 529–540, https://doi.org/10.1016/S0012-821X(02)01124-X.

Filbrandt, J.B., Al-Dhahab, S., Al-Habsy, A., Harris, K., Keating, J., Al-mahruqi, S., Ozkaya, S.I., Richard, P.D., and Robertson, T., 2006, Kinematic interpretation and structural evolution of North Oman, Block 6, since the Late Cretaceous and implications for timing of hydrocarbon migration into Cretaceous reservoirs: GeoArabia, v. 11, no. 786, p. 97–115.

Fleet, A.J., and Robertson, A.H.F., 1980, Ocean-ridge metalliferous and pelagic sediments of the Semail nappe, Oman: Journal of the Geological Society of London, v. 137, no. 4, p. 403–422, https://doi.org/10.1144/gsjgs.137.4.0403.

Forbes, G.A., Jansen, H.S.M., and Schreurs, J., 2010, Lexicon of Oman—Subsurface Stratigraphy—Reference Guide to the Stratigraphy of Oman's Hydrocarbon Basins: GeoArabia Special Publication 5: Manama, Bahrain, Gulf PetroLink, 371 p.

Fournier, M., Lepvrier, C., Razin, P., and Jolivet, L., 2006, Late Cretaceous to Paleogene post-obduction extension and subsequent Neogene compression in the Oman Mountains: GeoArabia, v. 11, no. 4, p 17–40.

Glennie, K.W., Boeuf, M.G.A., Hughes Clarke, M.W., Moody-Stuart, M., Pilaar, W.F.H., and Reinhardt, B.M., 1973, Late Cretaceous nappes in Oman Mountains and their geologic evolution: The American Association of Petroleum Geologists Bulletin, v. 57, p. 5–27.

Glennie, K.W., Boeuf, M.G.A., Hughes-Clarke, M.W., Moody-Stuart, M., Pilaar, W.F.H., and Reinhardt, B.M., 1974, Geology of the Oman Mountains: Verhandelingen van het Koninklijk, Nederlands Geologisch-Mijnbouwkundig Genootschap, v. 31, 423 p.

Hanna, S.S., 1990, The Alpine deformation of the Central Oman Mountains, *in* Robertson, A.H.F., Searle, M.P., and Ries, A.C., eds., The Geology and Tectonics of the Oman Region: Geological Society of London Special Publication 49, p. 341–359, https://doi.org/10.1144/GSL.SP.1992.049.01.21.

Hansman, R.J., Ring, U., Thomson, S.N., den Brock, B., and Stübner, K., 2017, Late Eocene uplift of the Al Hajar Mountains, Oman, supported by stratigraphic and low-temperature thermochronology: Tectonics, v. 36, no. 12, p. 3081–3109, https://doi.org/10.1002/2017TC004672.

Hutchison, I., Louden, K.E., White, R.S., and Von Herzen, R.P., 1981, Heat flow and age in the Gulf of Oman: Earth and Planetary Science Letters, v. 56, p. 252–262, https://doi.org/10.1016/0012-821X(81)90132-1.

Jung, S., and Ali, M., 2018, Petroleum Geology and Hydrocarbon Potential of the Eastern Offshore United Arab Emirates: AAPG/Middle East GTW Carbonate Reservoirs of the Middle East and Their Future Challenges, Abu Dhabi, UAE: Jan 30-Feb 1 2018: AAPG Datapages/Search and Discovery Article #90318.

Le Métour, J., Villey, M., and de Gramont, X., 1986, Explanatory notes Geological map of Masqat Sheet NF 40-4A Ministry of Petroleum and Minerals Sultanate of Oman.

Lippard, S.J., Shelton, A.W., and Gass, I.G., 1986, The Ophiolite of Northern Oman: Geological Society of London Memoir 11, 178 p.

Manghnani, M.H., and Coleman, R.G., 1981, Gravity profiles across the Samail ophiolite, Oman: Journal of Geophysical Research, v. 86, B4, p. 2509–2525, https://doi.org/10.1029/JB086iB04p02509.

Mann, A., Hanna, S.S., and Nolan, S.C., 1990, The post-Campanian tectonic evolution of the central Oman Mountains: Tertiary extension of the eastern Arabian margin, *in* Robertson, A.H.F., Searle, M.P., and Ries, A.C., eds., The Geology and Tectonics of the Oman Region: Geological Society of London Special Publication 49, p. 549–563, https://doi.org/10.1144/GSL.SP.1992.049.01.33.

Masse, J.P., Borgomano, J., and Al-Maskiry, S., 1997, Stratigraphy and tectonosedimentary evolution of a late Aptian–Albian carbonate margin: The northeastern Jebel Akhdar (Sultanate of Oman): Sedimentary Geology, v. 113, p. 269–280, https://doi.org/10.1016/S0037-0738(97)00065-1.

Mattern, F., and Scharf, A., 2018, Postobductional extension along and within the Frontal Range of the Eastern Oman Mountains: Journal of Asian Earth Sciences, v. 154, p. 369–385, https://doi.org/10.1016/j.jseaes.2017.12.031.

Nicolas, A., Boudier, F., and Ildefonse, B., 1996, Variable crustal thickness in the Oman ophiolite: Implication for oceanic crust: Journal of Geophysical Research, v. 101, p. 17,941–17,950, https://doi.org/10.1029/96JB00195.

Ninkabou, D., Agard, P., Nielsen, C., Smit, J., Gorini, C., Rodriguez, M., Haq, B., Chamot-Rooke, N., Weidle, C., and Ducassou, C., 2021, Structure of the offshore obducted Oman margin: Emplacement of Semail ophiolite and role of tectonic inheritance: Journal of Geophysical Research: Solid Earth, https://doi.org/10.1029/2020JB020187.

Nolan, S.C., Skelton, P.W., Clissold, B.P., and Smewing, J.D., 1990, Maastrichtian to early Tertiary stratigraphy and palaeogeography of the Central and Northern Oman Mountains, *in* Robertson, A.H.F., Searle, M.P., and Ries, A.C., eds., The Geology and Tectonics of the Oman

Region: Geological Society Special Publication 49, p. 495–519, https://doi.org/10.1144/GSL.SP.1992.049.01.31.
Platt, J.P., Leggett, J.K., Young, J., Raza, H., and Alam, S., 1985, Large-scale underplating in the Makran accretionary prism, southwest Pakistan: Geology, v. 13, p. 507–511, https://doi.org/10.1130/0091-7613(1985)13<507:LSUITM>2.0.CO;2.
Poupeau, G., Saddiqi, O., Michard, A., Goffé, B., and Oberhänsli, R., 1998, Late thermal evolution of the Oman Mountains subophiolitic windows: Apatite fission-track thermochronology: Geology, v. 26, p. 1139–1142, https://doi.org/10.1130/0091-7613(1998)026<1139:LTEOTO>2.3.CO;2.
Rabu, D., Béchennec, F., Beurrier, M., and Hutin, G., 1986, Geological Map of Nakhl Sheet NF 40-3E Scale 1:100,000 with Explanatory Notes. Directorate General of Minerals, Oman Ministry of Petroleum and Minerals.
Rabu, D., Nehlig, P., and Roger, J., 1993, Stratigraphy and structure of the Oman Mountains: Bureau de Recherches Geologiques et Minieres, v. 221.
Racey, A., 1995, Lithostratigraphy and larger foraminiferal (nummulitid) biostratigraphy of the Tertiary of northern Oman: Microplaeontology, v. 41, p. 1–123, https://doi.org/10.2307/1485849.
Racz, L., 1979, Paleocene carbonate development of Ras al Hamra, Oman: Bulletin des Centres de Recherches Exploration Elf, 3.2, p. 767–779.
Ravaut, P., Bayer, R., Hassani, R., Rousset, D., and Yahya'ey, A.A., 1997, Structure and evolution of the northern Oman margin: gravity and seismic constraints over the Zagros-Makran-Oman collision zone: Tectonophysics, v. 279, p. 253–280, https://doi.org/10.1016/S0040-1951(97)00125-X.
Ravaut, P., Carbon, D., Ritz, J.F., Bayer, R., and Philip, H., 1998, The Sohar Basin, Western Gulf of Oman: Description and mechanisms of formation from seismic and gravity data: Marine and Petroleum Geology, v. 15, p. 359–377, https://doi.org/10.1016/S0264-8172(98)00055-5.
Ricateau, R., and Riché, P.H., 1980, Geology of the Musandam peninsula (Sultanate of Oman) and its surroundings: Journal of Petroleum Geology, v. 3, no. 2, p. 139–152, https://doi.org/10.1111/j.1747-5457.1980.tb00979.x.
Rioux, M.E., Gerber, J.M., Searle, M.P., Miyashita, S., Adachi, Y., Bowring, S.A., Keleman, P.B., and Bauer, A.J., 2016, Melting of the subducted slab and mantle wedge during subduction initiation below the Semail (Oman-UAE) ophiolite: San Francisco, American Geophysical Union, Fall Meeting, 12-16 December, https://agu.confex.com/agu/fm16/meetingapp.cgi/Paper/181536.
Robertson, A., 1988, Late Cretaceous chemical sediments related to a carbonate platform foreland basin transition in the Oman Mountains: Sedimentary Geology, v. 57, p. 1–15, https://doi.org/10.1016/0037-0738(88)90015-2.
Robertson, A., 1987a, The transition from a passive margin to an Upper Cretaceous foreland basin related to ophiolite emplacement in the Oman Mountains: Geological Society of America Bulletin, v. 99, p. 633–653, https://doi.org/10.1130/0016-7606(1987)99<633:TTFAPM>2.0.CO;2.
Robertson, A.H.F., 1987b, Upper Cretaceous Muti Formation: Transition of a Mesozoic carbonate platform to a foreland basin in the Oman Mountains: Sedimentology, v. 34, p. 1123–1142, https://doi.org/10.1111/j.1365-3091.1987.tb00596.x.
Robertson, A.H.F., and Searle, M.P., 1990, The northern Oman Tethyan continental margin: Stratigraphy, structure, concepts and controversies, *in* Robertson, A.H.F, Searle, M.P., and Ries, A., eds., The Geology and Tectonics of the Oman Region: Geological Society of London Special Publication 49, p. 3–25, https://doi.org/10.1144/GSL.SP.1992.049.01.02.
Robertson, A.H.F., and Woodcock, N.H., 1983, Genesis of the Batinah mélange above the Semail ophiolite, Oman: Journal of Structural Geology, v. 5, p. 1–17, https://doi.org/10.1016/0191-8141(83)90003-2.
Rodriguez, M., Huchon, P., Chamot-Rooke, N., Fournier, M., and Delescluse, M., 2016, Tracking the Paleogene India-Arabia plate boundary: Marine and Petroleum Geology, v. 72, p. 336–358, https://doi.org/10.1016/j.marpetgeo.2016.02.019.
Roger, J., Bourdillon, C., Razin, Ph., Le Callonnec, L., Renard, M., Aubry, M.P., Platel, J.-P., Wyns, R., and Bonnemaison, M., 1998, Modifications des paléoenvironnements et des associations biologiques autour de la limite Crétacé-Tertiaire dans les montagnes d'Oman: Bulletin de la Société Géologique de France, v. 169, no. 2, p. 255–270.
Saddiqi, O., Michard, A., Goffe, B., Poupeau, G., and Oberhansli, R., 2006, Fission-track thermochronology of the Oman Mountains continental windows, and current problems of tectonic interpretation: Bulletin de la Société Géologique de France, v. 177, no. 3, p. 127–134, https://doi.org/10.2113/gssgfbull.177.3.127.
Scharf, A., Mattern, F., Moraetis, D., Callegari, I., and Weidle, C., 2019, Postobductional kinematic evolution and geomorphology of a major regional structure—The Semail Gap Fault zone (Oman Mountains): Tectonics, v. 38, p. 2756–2778, https://doi.org/10.1029/2019TC005588.
Scharf, A., Sudo, M., Pracejus, B., Mattern, F., Callegari, I., Bauer, W., and Scharf, K., 2020, Late Lutetian (Eocene) mafic intrusion into shallow marine platform deposits north of the Oman Mountains (Rusayl Embayment) and its tectonic significance: Journal of African Earth Sciences, v. 170, p. 103941, https://doi.org/10.1016/j.jafrearsci.2020.103941.
Schlüter, M., Steuber, T., Parente, M., and Mutterlose, J., 2008, Evolution of a Maastrichtian–Paleocene tropical shallow-water carbonate platform (Qalhat, NE Oman): Facies, v. 54, p. 513–527, https://doi.org/10.1007/s10347-008-0150-8.
Schulp, A.S., Hanna, S.S., Hartman, A.F., and Jagt, J.W.M., 2000, A Late Cretaceous theropod caudal vertebra from the Sultanate of Oman: Cretaceous Research, v. 21, p. 851–856, https://doi.org/10.1006/cres.2000.0235.
Searle, M.P., 1985, Sequence of thrusting and origin of culminations in the northern and central Oman Mountains: Journal of Structural Geology, v. 7, p. 129–143, https://doi.org/10.1016/0191-8141(85)90127-0.
Searle, M.P., 2007, Structural geometry, style and timing of deformation in the Hawasina Window, Al Jabal al Akhdar and Saih Hatat culminations, Oman Mountains: GeoArabia, v. 12, no. 2, p. 99–132.
Searle, M.P., Warren, C.J., Waters, D.J., and Parrish, R.R., 2004, Structural evolution, metamorphism and restoration of the Arabian continental margin, Saih Hatat region, Oman Mountains: Journal of Structural Geology, v. 26, no. 3, p. 451–473, https://doi.org/10.1016/j.jsg.2003.08.005.
Shelton, A.W., 1990, The interpretation of gravity data in Oman: Constraints on the ophiolite emplacement mechanism, *in* Robertson, A.H.F., Searle, M.P., and Ries, A.C., eds., The Geology and Tectonics of the Oman Region: Geological Society of London Special Publication 49, p. 459–471, https://doi.org/10.1144/GSL.SP.1992.049.01.29.
Skelton, P., Nolan, S.C., and Scott, R.W., 1990, The Maastrichtian transgression onto the northwestern flank of the Proto-Oman Mountains: sequences of rudist-bearing beach to open shelf facies, *in* Robertson, A.H.F., Searle, M.P., and Ries, A.C., eds., The Geology and Tectonics of the Oman Region: Geological Society of London Special Publication 49, p. 521–547, https://doi.org/10.1144/GSL.SP.1992.049.01.32.
Terken, J.M.J., 1999, The Natih petroleum system of North Oman: GeoArabia, v. 4, no. 2, p. 157–180.
Uchupi, E., Swift, S.A., and Ross, D.A., 2002, Tectonic geomorphology of the Gulf of Oman basin, *in* Clift, P.D., Kroon, D., Gaedicke, C., and Craig, J., eds., The Tectonic and Climate Evolution of the Arabian Sea Region: Geological Society of London Special Publication 195, p. 37–69, https://doi.org/10.1144/GSL.SP.2002.195.01.04.
Vigny, C., Huchon, P., Ruegg, J.C., Khanbari, K., and Asfaw, L.M., 2006, Confirmation of Arabia plate slow motion by new GPS data in Yemen: Journal of Geophysical Research, v. 111, B02402, https://doi.org/10.1029/2004JB003229.
Villey, M., Le Métour, J., and De Gramont, X., 1986a, Geological Map of Fanjah Sheet NF 40–3F. Scale 1:100,000 with Explanatory Notes. Directorate General of Minerals, Oman Ministry of Petroleum and Minerals.
Villey, M., De Gramont, X., and Le Métour, J., 1986b, Geological Map of Sib Sheet NF 40–3C Scale 1:100,000 with Explanatory Notes. Directorate General of Minerals, Oman Ministry of Petroleum and Minerals.
Warburton, J., Burnhill, T.J., Graham, R.H., and Isaac, K.P., 1990, The evolution of the Oman Mountains foreland basin, *in* Robertson, A.H.F., Searle, M.P., and Ries, A.C., eds., The Geology and Tectonics of the Oman Region: Geological Society of London Special Publication 49, p. 419–427, https://doi.org/10.1144/GSL.SP.1992.049.01.26.
Warren, C.J., Parrish, R.R., Searle, M.P., and Waters, D.J., 2003, Dating the subduction of the Arabian continental margin beneath the Semail ophiolite, Oman: Geology, v. 31, p. 889–892, https://doi.org/10.1130/G19666.1.
Warren, C.J., Parrish, R.R., Waters, D.J., and Searle, M.P., 2005, Dating the geologic history of Oman's Semail ophiolite: Insights from U-Pb geochronology: Contributions to Mineralogy and Petrology, v. 150, p. 403–422, https://doi.org/10.1007/s00410-005-0028-5.
Whitbread, T., Nicholson, T., and Owens, W., 2001, Structural evolution of a detached delta system—the Vicksburg of south Texas: The Leading Edge, no. 10, p. 1106–1117, https://doi.org/10.1190/1.1487240.
White, R.S., 1982, Deformation of the Makran accretionary sediment prism in the Gulf of Oman (North-West Indian Ocean), *in* Leggett, J.K., ed., Trench-Forearc Geology: Sedimentation and Tectonics on Modern and Ancient Active Plate Margins: Geological Society of London Special Publication 10, p. 357–372, https://doi.org/10.1144/GSL.SP.1982.010.01.24.
White, R.S., and Ross, D.A., 1979, Tectonics of the western Gulf of Oman: Journal of Geophysical Research, v. 84, p. 3479–3489, https://doi.org/10.1029/JB084iB07p03479.
Woodcock, N.H., and Robertson, A.H.F., 1982, The upper Batinah Complex, Oman: allochthonous sediment sheets above the Semail ophiolite: Canadian Journal of Earth Sciences, v. 19, p. 1635–1656, https://doi.org/10.1139/e82-140.